IGNITION DYNAMICS OF DOUBLE BASE PROPELLANTS

Aerospace and Mechanical Sciences Report
No. 1150

by

M. Summerfield, L. H. Caveny,
T. J. Ohlemiller and L. DeLuca

Performed under
U.S. Army Research Office in Durham
Grant DA-ARO-D-31-124-72-G119

JANUARY 1974

PRINCETON UNIVERSITY

DEPARTMENT OF
AEROSPACE AND MECHANICAL SCIENCES

SECURITY CLASSIFICATION OF THIS PAGE (When Data Entered)

REPORT DOCUMENTATION PAGE		READ INSTRUCTIONS BEFORE COMPLETING FORM
1. REPORT NUMBER	2. GOVT ACCESSION NO. AD-A132154	3. RECIPIENT'S CATALOG NUMBER
4. TITLE (and Subtitle) IGNITION DYNAMICS OF DOUBLE BASE PROPELLANTS		5. TYPE OF REPORT & PERIOD COVERED Scientific Interim
		6. PERFORMING ORG. REPORT NUMBER AMS Report No. 1150
7. AUTHOR(s) M. Summerfield, L. H. Caveny, T. J. Ohlemiller and L. DeLuca		8. CONTRACT OR GRANT NUMBER(s) DA-ARO-D-31-124-72-G119
9. PERFORMING ORGANIZATION NAME AND ADDRESS Aerospace & Mechanical Sciences Dept. Princeton University Princeton, New Jersey 08540		10. PROGRAM ELEMENT, PROJECT, TASK AREA & WORK UNIT NUMBERS
11. CONTROLLING OFFICE NAME AND ADDRESS U.S. Army Research Office Durham, North Carolina		12. REPORT DATE January 1974
		13. NUMBER OF PAGES viii + 39
14. MONITORING AGENCY NAME & ADDRESS(if different from Controlling Office) Ballistic Research Laboratories Aberdeen Proving Grounds, Md.		15. SECURITY CLASS. (of this report) Unclassified
		15a. DECLASSIFICATION/DOWNGRADING SCHEDULE

16. DISTRIBUTION STATEMENT (of this Report)
Approved for public release; distribution unlimited.

17. DISTRIBUTION STATEMENT (of the abstract entered in Block 20, if different from Report)

18. SUPPLEMENTARY NOTES
Requests for additional copies should be made to the National Technical Information Service, U.S. Department of Commerce, Springfield, Va. 22151

19. KEY WORDS (Continue on reverse side if necessary and identify by block number)

Solid propellant ignition
Radiative ignition
Arc image furnace
Laser (CO_2) heating
Mathematical model of ignition
Composite propellants
Double base propellants
Platonized propellants
Sq. Cm/Sec

20. ABSTRACT (Continue on reverse side if necessary and identify by block number)

Ignition and transient combustion characteristics of composite propellants (AP or HMX types) and double base propellants (NC/NG and NC/MTN types) were classified by their responses to strong radiant heating (5 to 100 cal/cm^2-sec) from laser and arc sources. Ignition times (go/no-go measurements) are significantly different for the two classes of propellant and are affected greatly by addition of carbon powder and/or combustion catalysts. The results reveal several important generalizations. With the arc furnace the opacifiers in

Continued - over

DD FORM 1 JAN 73 1473 EDITION OF 1 NOV 65 IS OBSOLETE

the condensed phase can lower the ignition times as much as tenfold. For double base propellants, the time to the IR emission level corresponding to the onset of surface decomposition is independent of pressure and O_2 concentration, whereas the time to sustained flame (go/no-go test) depends on both. A mathematical model for ignition and the nonsteady burning following ignition, employing the nonsteady heat feedback function of Zeldovich, was solved and shown to predict quite well the same type of behavior as that found experimentally. The problem of relating convective ignition response (needed for rocket and other applications) to radiative ignition test results was shown to be complicated by the inherent characteristics of radiation experiments, i.e., propellant reflectivity and transparency, slow kinetics in the cool gas phase, dynamic extinction during deradiation, and spatial variation of radiation flux on the target surface.

TABLE OF CONTENTS

LIST OF TABLES

LIST OF FIGURES

SUMMARY

Ignition and transient combustion characteristics of composite propellants (AP or HMX types) and double base propellants (NC/NG and NC/MTN types) were classified by their responses to strong radiant heating (5 to 100 cal/cm^2-sec) from laser and arc sources. These results are providing guidelines that permit the designer to maximize igniter effectiveness with minimal development testing. Ignition times (go/no-go measurements) are significantly different for the two classes of propellant and are affected greatly by addition of carbon powder and/or combustion catalysts. The results reveal several important generalizations. With the arc furnace the opacifiers in the condensed phase can lower the ignition times as much as ten-fold. For double base propellants, the time to the IR emission level corresponding to the onset of surface decomposition is independent of pressure and O_2 concentration, whereas the time to sustained flame (go/no-go test) depends on both.

The dynamic response of a solid propellant to a rapidly decreasing radiation flux is representative of the general class of transient responses of heterogeneous flames to rapid disturbances. The response of double base propellants to roughly square wave radiation pulses was examined. When such pulses are used to ignite propellants, they may in some cases produce a flame which persists for whatever duration the pulse persists, but which extinguishes as soon as the pulse stops. This tendency to extinction upon deradiation was found to be lessened by increased pressure, increased deradiation time and addition of carbon powder. The effect disappears entirely when burning rate catalysts are added. This extinction response upon deradiation is not limited to the ignition situation; it was shown experimentally that a steadily burning propellant can be extinguished by a radiation pulse of appropriate magnitude, duration, and speed of cut-off. It was shown that this dynamic extinction behavior results from an imbalance in the heat fluxes to and from the burning surface during deradiation.

A mathematical model for ignition and the nonsteady burning following ignition, employing the nonsteady heat feedback function of Zeldovich, was solved and shown to predict quite well the same type of behavior as that found experimentally.

The problem of relating convective ignition response (needed for rocket and other applications) to radiative ignition test results was shown to be complicated by the inherent characteristics of radiation experiments, i.e., propellant reflectivity and transparency, slow kinetics in the cool gas phase, dynamic extinction during deradiation, and spatial variation of radiation flux on the target surface.

Based on research sponsored by the U. S. Army Research Office in Durham under Grant DA-ARO-D-31-124-72-G119 and monitored by the Ballistic Research Laboratories, Aberdeen Proving Ground, Md.

NOTE: This material is to be published in a volume on AMC Fundamentals of Ignition Task.

I. INTRODUCTION

This research is elucidating the physical and chemical factors that control ignition of double base propellants. The knowledge gained will provide rational guidelines for the interior ballistician in designing igniters and for the propellant formulator in tailoring ignition characteristics to specific applications. Emphasis is on (1) detailed experimental investigations of the processes that occur at and near the propellant surface, (2) the connection between the ignitability of a propellant and its other combustion characteristics, and (3) on quantifying the peculiarities of radiative ignition in comparison with convective ignition. As a result of this research the ignition trends of different propellant types (e.g., composite vs double base) and of several modified propellants (e.g., noncatalyzed vs catalyzed double base and transparent vs opaque propellants) are being rationalized in terms of basic differences in the structure of the deflagration wave in the solid and gas phases (see Ref. 1). The problem of flame retention during the ignition transient of solid propellants is being investigated both analytically and experimentally. Of particular interest are the factors that determine whether sustained ignition (steady burning) or extinction ensues when the ignition stimulus is removed. In general this extinction may result from two types of causes, insufficient flame development (premature withdrawal of the ignition stimulus) or dynamic effects attending the actual withdrawal of the stimulus (despite full flame development); one segment of the present work is focused on this latter type of cause (see Ref. 2).

A convenient format for presenting and analyzing radiative ignition results is a logarithmic plot of heating time vs incident radiant flux (called an ignition map). This is constructed from tests in which a propellant sample is subjected to a constant flux for a fixed time (square-wave pulse). Boundaries on such a map define regions of differing propellant response (no effect, gasification, flame development, etc.).

In previous studies, ignition maps with complex boundaries have stimulated discussion and analyses of the underlying combustion mechanisms. For example, Price and co-workers[3] developed ignition maps which showed interactions between condensed phase reactions, gas phase reactions, free convection, and dilution of flame zone by chamber gases. Also, Lenchitz and co-workers[4] discovered several difficult to explain ignition trends during their examination of thin nitrocellulose films. In the spirit of this research, complex interactions of the ignition trends are welcomed because they are often useful in deducing information about the ignition and transient burning processes.

II. GENERALIZED IGNITION MAP

As a means of efficiently presenting and interpreting the experimental results, we have chosen to describe the expected ignition events and limits prior to presenting the data. Figure 1 shows a traverse of event limits (boundary points) on an ignition map. The traverse is at a fixed value of pressure and radiant flux intensity. The events traversed on the ignition map are:

L_{1a} the surface is heated to the point that it is being gasified and a carbonaceous layer may form on the surface but vigorous exothermic reactions are not occurring. For any lesser heating time, no visible effect is seen.

L_{1b} either gas phase or surface reactions begin to accelerate rapidly (as indicated by the appearance of a detectable IR signal from the gas just above the sample surface).

L_{1c} incipient flame appears.

L_{1d} self-sustaining ignition.

L_2 rapid deradiation (of some propellants) between limits L_2 and L_3 results in dynamic extinguishment.

L_3 sustained combustion following deradiation (assured by flame spreading away from the target area of radiant heating).

Limits L_{1d}, L_2, and L_3 must be established by go/no-go testing.

The limits L_{1d}, L_2, and L_3 are very specific limits whose positions (and even existence) are strongly dependent on propellant type and test conditions (i.e., pressure, atmosphere, deradiation time, spatial distribution of radiant beam, etc.). Furthermore, as indicated on Fig. 1, the limits L_{1a}, L_{1b}, L_{1c}, and L_{1d} may not be detectable as four individual limits since two or more of the limits may occur nearly simultaneously, depending on pressure, heat flux, and atmosphere. When all four limits occur nearly simultaneously, the limits will be referred to simply as the L_1 limit. The implication is that a self-sustaining flame develops very quickly the moment the propellant begins to gasify.

In terms of limits shown on Fig. 1, the conditions for ignition may be treated as two essential conditions. The first is the development of the initial exothermic reactions, (i.e., limits L_{1a}, L_{1b}, and L_{1c}) partially within the propellant surface reaction layer and partially in the adjacent gas phase boundary layer. Corresponding quantitative theories have evolved to treat this condition: one of the earliest was the theory of Frazer and Hicks[5] which dealt with the condensed phase; detailed physical modeling of the flame has come from Princeton (e.g., Ref. 6 and 8); and there have been other contributions (e.g., Ref. 9-14). Several of the models were reviewed in Ref. 14. The second condition is focused on the final stage of the surface reactions and flame development and emphasizes the conditions for flame retention after the heat source is removed, i.e., limit L_{1d}. We call this second condition a late-stage type of theory, in contrast to the first conditions which we call the early-stage type of theory. In the late stage, attention is focused on matching of the heat feedback from a quasi-steady (fully developed) flame to the heating rate required to prepare the condensed phase for burning. There are many instances in which the appearance of visible flame does not insure self-sustaining combustion.

In our experimental and theoretical studies we have analyzed conditions under which a nitrocellulose double base (DB) propellant can be brought successfully to ignition in terms of the late stage definition (self-sustaining combustion following deradiation, i.e., L_{1d} is crossed), but, if the heating time is increased beyond L_2, the propellant will fail to retain the flame following rapid deradiation and the propellant stops burning. This dynamic extinction occurs because the heat flux from the flame is too low to maintain (during the thermal relaxation period) the energy required by the condensed phase immediately following the overdriven situation of radiation assisted burning. To our knowledge to obtain such a dynamic extinguishment, radiant heating following the L_{1d} limit must drive the burning rate above the steady state burning rate. The L_2 limit is discussed in Section V.

The upper limit, L_3, above which dynamic extinction does not occur, corresponds to the time required for flame to spread over the irradiated surface beyond the target area of direct exposure. Under these conditions,

the dynamic extinction (following rapid deradiation) is restricted to the portion of the propellant surface exposed to the radiant beam; the unperturbed deflagration wave surrounding the target area can reignite the entire surface. Since the long exposure times cause the one-dimensionality of the ignition process to break down, the subsequent disappearance of dynamic extinction is referred to on the ignition maps as "3-D reignition".

Measurement of the time to a prescribed level of IR emission from the propellant surface reveals that the appearance of the (incipient) flame corresponds to a well defined boundary, L_{1c}. Significantly, the beginning (L_{1b}) of the rapidly accelerating infrared (IR) signal from the propellant surface region is independent of pressure and O_2 concentration, but whether and how rapidly strong surface reactions occur depend on both. Therefore, the appearance of initial surface reaction (L_{1b} limit), is controlled by condensed phase and surface processes and can be described by simple thermal theory. However, as previously pointed out, neither the appearance of an incipient flame (L_{1c} limit) nor condensed phase thermal theories (L_{1a} or L_{1b} limits) are in general adequate for declaring that sustained ignition (crossing of L_{1d} limit) will occur. In particular situations (e.g., high pressure and low heat flux), the condensed phase thermal profile is well established and the propellant is able to provide vigorous energy feedback to the surface and rapid flame development occurs; the requirements for a self-sustaining flame are automatically satisfied when a prescribed surface temperature is achieved. In this case, no late-stage theory is needed and the ignition is assured by crossing the L_{1a} limit.

III. SUMMARY OF EXPERIMENTAL PROCEDURE

The two radiative sources used in the study are an arc image furnace (Fig. 2a) and a CO_2 laser (Fig. 2b). The Xenon lamp in the arc image apparatus provides the arc whose image is focused at the surface of the propellant sample (2.6 mm in diameter). The intensity of the radiant flux (up to 120 cal/cm^2-sec) is controlled in a diseontinuous manner by inserting attenuation screens (e.g., stainless steel mesh) into the optical path. The CO_2 laser (see Ref. 15 for more details) provides a continuous emission at 10.6μ with a maximum heat flux of 100 cal/em^2-sec. However, the radiant beam is spatially nonuniform (e.g., at 36 eal/cm^2-see the time for the onset of first gasification may vary by 10-15% over the 3 by 3 mm target area). The basic difference in the speetral emissions from the Xenon arc lamp and from the CO_2 laser is shown in Fig. 2b.

It follows from the discussion in Section II that the appropriate experimental method for rating the ignitability of propellants is the go/no-go type of test rather than detecting a flame during the continuous radiation type of test, since the appearanee of the ineipient flame (as indicated by either IR or photo detectors) is often only a step in the overall ignition transient.

The duration and rate cf termination of the radiant pulse of known intensity are controlled by two high speed, iris type shutters which operate within 1 msec. The speed of the shutter systems is a very important parameter, differences on the order of one msec in the deradiation time can shift the time of the L_2 boundary 50% (see Fig. 3 in Ref. 2). The point-by-point nature of the go/no-go data is illustrated on Figs. 3, 4, 6, 12 and 15 which show a few of the points closest to the boundary. Statistical treatments were not applied to the data. Uncertainties concerning a boundary were reduced by conducting additional tests in the vicinity of the boundary. Where necessary as many as) tests

were used to define a boundary. A typical boundary was defined with 20 tests. The results are plotted as the log of radiative heating time vs log of intensity of the incident radiant flux. To permit direct comparisons, all of the results are plotted on the same grid.

Most of the propellants considered were tested with the arc and the laser at 5, 11, and 21 atm (either air or N_2) and at radiant flux intensities up to 100 cal/cm^2-sec. The response of the propellant to the radiant pulse is observed both as a global result of ignition or no ignition and as detailed processes of gasification, incipient flame, and well developed flame. For selected tests, high speed (1000 frame/sec) shadowgraph and color movies, and fine thermocouples recorded the ignition sequence.

The standard sample geometry is a cylinder 2.6 mm in diameter which is smaller than the 3 x 3 mm region heated by the laser. The surfaces were freshly cut with a razor blade a few minutes before the test. The propellants for which ignition maps were measured are listed in Table I. Propellants 9 and 10 are referred to as catalyzed DB propellants since they contain lead and copper salts that produce increased burning rates.[16]

Overall IR emissions from the propellant surface region were observed during continuous radiation assisted ignition experiments carried out in the laser apparatus for the same experimental parameters as used for the go/no-go type of experiments. For each condition, two times were observed during the ignition transient: (1) the time of appearance of surface reactions, at which the IR detector senses a first faint emission of radiation somewhere near the surface, and (2) the time of strong surface reactions, at which a given level of IR emission from the surface region is reached. The IR detector is a photoconductor made of gold-doped germanium. It is positioned so that it detects radiation from the surface region through an optical path consisting of two Irtran 2 windows and a front surface aluminum coated mirror. As shown in Fig.2b, the spectral range of the overall IR detector system includes the surface emissions of interest (i.e., approximates surface temperatures of AP composite and DB propellants) but responds very weakly to the 10.6μ emission of the laser. The IR detector signal level that corresponds to the first detectable surface reaction (L_{1b} limit) was established by high speed motion pictures and by examining surfaces of relics from no-go tests.

IV. COMPARATIVE ANALYSIS OF IGNITION CHARACTERISTICS

Propellants and test conditions were selected that emphasized particular ignition events and thermal processes. As a means of efficiently presenting and interpreting the results, we have related the measured boundaries to the limits presented in Fig. 1. This section consists of five subtopics that employ the data to elucidate a range of characteristics. The scope of the tests is summarized in Table II . Since the objective of this section is to present and describe data from a wide variety of propellants and test conditions, the detailed comparisons require that the reader make repeated references to the figures.

A. Observations by Propellant Class

A comparison of the relative ignitability (under arc image heating) of the several propellant classes is given in Fig. 3. Under the 21 atm conditions shown on Fig. 3, the ignition limits are straight lines over the indicated range of heat fluxes. At lower pressures (e.g., 5 atm), several of the limit lines are not straight and a direct comparison of the propellants is more difficult. Most prominently, the HMX/PU propellants are the most resistant to ignition. The next most resistant

propellants are the AP composite propellants. The opacified NC double base propellants (i.e., propellants containing particulate carbon) are clearly the easiest to ignite. These trends are consistent with the burning surface temperatures of the three propellant types (i.e., 260 to 340°C for NC[16], 700 to 800 for AP composite,[17] and 1050 for HMX composite,[18]) and with the reflectivities and extinction coefficients of Table III.

The very large differences in the ignition times will be used here as a means of deducing information concerning the combustion processes of the several propellant classes.

For tests conducted in N_2 at pressures between 5 and 21 atm, each propellant class demonstrates distinct characteristics:

1. AP composite propellants (see Fig. 4) are characterized by a single L_1 limit (see Fig. 1) between nonignition and sustained ignition regions, i.e., the L_{1a}, L_{1b}, L_{1c} and L_{1d} limits merge into one. The boundary is a straight line whose location and slope are independent of pressure but depend to some extent on radiation penetration below the surface. (Below 5 atm, pressure dependence becomes pronounced, particularly in the high intensity range.)[3]
2. Catalyzed DB propellants (see Fig. 5) are characterized by the existence of clearly defined L_{1a} and L_{1d} limits. As pressure increases, the L_{1d} limit becomes a single straight line and the non-self-sustaining flame region between the L_{1a} and L_{1d} limits decreases until it is eliminated.
3. Noncatalyzed propellants tested in the laser ignition apparatus (Fig. 6) have a single L_{1d} limit between nonignition and sustained ignition regions. Moreover, noncatalyzed DB propellants can be extinguished by rapid removal of the laser radiant beam. (Defined by the L_2 limit.)

The results obtained from tests of HMX/PU propellants (which are known to be resistant to ignition) in the arc image ignition apparatus are shown in Fig. 7. In an N_2 atmosphere, propellants 11 and 13 at 5 and 11 atm could not be ignited using exposure times up to 500 msec; at 21 atm relatively long exposure times are required to achieve ignition. Ignition of propellant 12 which contains 10% oxamide (a burning rate suppressant which decomposes endothermically on the surface) was very difficult. For example, at 50 cal/cm^2-sec of radiant flux and at 11 atm of N_2, exposure times on the order of one second were required. The ignitability of HMX composite propellants in air was explored only for propellant 12. The propellant ignited easily in air but a pressure dependent behavior was observed.

When propellants 11, 12, and 13 are tested in the laser apparatus there is a marked decrease in the ignition time which is probably a result of the 10.6μ radiation from the laser being absorbed at the surface, whereas the 0.5 to 1.5μ radiation from the arc image may be partially attenuated by reflection from the surface as well as transmitted below the propellant surface. Preliminary results in the laser ignition apparatus are: (1) propellant 11 ignited in nitrogen at 21 atm (marginally at 10 atm) and in air at 5 atm; (2) propellant 12 was not ignitable in N_2, but does ignite at 5 atm in air; (3) propellant 13 is ignitable in N_2 at 21 atm; in air, it is ignitable at 5 atm. Again, a slight pressure dependence is observed in air.

The very fuel rich, propellant 4, behaved as a conventional AP composite propellant at 11 and 21 atm (see Fig. 4). The value of the slope

(-2) indicates that the penetration of radiation below the surface is negligible. Thus, for tests conducted at 11 and 21 atm, boron appears to act as an inert opacifier with no major effect on the ignition behavior of the propellant.

The differences in the flame structure of the several propellant classes were revealed by high speed shadowgraph movies (16 mm, 1000 frame/sec) taken during propellant ignition by the laser. For AP based propellants (Fig. 8), the movies show that first appearance of the incipient flame corresponds to the crossing of the go/no-go ignition boundary (L_1) and that soon afterward a thin flame develops strongly coupled to the surface. As clearly shown in Fig. 8, the incipient flame appears initially without the gasification period observed during the ignition of DB propellant (see Fig. 11). Movies of noncatalyzed DB propellants ignited at high pressure (21 atm) show that a distended visible flame develops, loosely coupled to the surface (see Fig. 11); the more closely surface-coupled fizz zone reactions emit no visible light.

A characteristic carbonaceous layer (Fig. 10) is observed when catalyzed DB propellants are ignited at low pressure ($\sim$ 4 atm). This is never observed for AP composite or noncatalyzed DB propellants; also, this is less pronounced when catalyzed DB propellants are ignited at high pressure (21 atm). Formation, growing, and emission of carbonaceous filaments on the surface occurring prior to the time of self-sustaining combustion appear to indicate a strong solid phase activity promoted by the catalysts. In all observed cases, the carbonaceous layer is a necessary precursor for self-sustaining combustion.

B. Effect of Catalyst in Double Base Propellants

Pressure sensitive L_{1d} boundaries (i.e., self-sustaining ignition) that are characteristic of catalyzed DB propellants are shown in Figs. 5 and 12 for propellants 9 and 10. Note that the behavior for arc image and laser heating is similar (see Fig. 5) and that dynamic extinction is not observed at any pressure (compare Figs. 5 and 11 with Figs. 6 and 14). The reproducibility of the strong IR signal from the surface region is better for the noncatalyzed DB propellants (Fig. 13) than for the catalyzed DB propellants (Fig. 14). The varied quantity, shape, and behavior of the hot carbonaceous residue that forms and sheds off of the catalyzed propellant surface (see Fig. 10) produces an irregular IR signal.

When catalysts are added, ignition by the laser is more easily achieved at 5 atm (compare propellant 10 results on Fig. 5 with propellant 7 results on Fig. 15).

The large difference in the arc image ignition boundaries of propellants 7 and 10 on Fig. 3 suggests two possibilities (1) under arc image heating the burning rate catalysts promote surface reactions at lower temperatures or (2) the finely divided PbSa and CuSa particles act as opacifiers to concentrate the arc image radiation at the propellant surface. Evidence for the former action is lacking. Indeed, under laser radiation, at 21 atm the L_{1a} limit for propellant 7 (Fig. 12) and propellant 10 (Fig. 11) almost coincide, which indicates that the catalysts do not accelerate the surface decomposition processes. Thus, the opacifying action (with respect to the arc image radiation) of the finely divided PbSa and CuSa as the explanation of the differences in the L_{1d} boundaries of propellants 7 and 10 (Fig. 3) appears to be reasonable (see Table III).

C. Effect of Atmosphere in Chamber

In general, the L_{1a} limits (i.e., first gasification) are not sensitive to pressure. The L_{1d} limits (i.e., self-sustaining ignition) of the nonmetallized AP composite propellants (Fig. 4) show no pressure sensitivity. The L_{1d} limits of the noncatalyzed DB propellants are not pressure sensitive in the laser but are pressure sensitive when tested in the arc-image (compare Figs. 6 and 12 with Fig. 15). The L_{1d} limits of catalyzed DB propellants have very similar pressure sensitivities in both the arc-image and the laser (see Fig. 5).

Most of the discussions presented so far concern experiments performed in N_2. Ignition results when air is the pressurizing gas in the laser ignition apparatus are presented in Figs. 13,14 and 16. Replacing N_2 with air has the following effects: (1) within the range of parameters investigated, pressure dependence is eliminated (e.g., the pressure dependencies of Figs. 11 and 15), (2) the dynamic extinction typical of the laser experiments (Fig. 8) is eliminated, and (3) the L_{1a} limits are essentially the same as found in tests performed in high pressure N_2, i.e., 21 atm.

The presence of atmospheric oxygen creates a vigorous secondary diffusion flame surrounding and overlapping the primary (and possibly) weak self-flame of the propellant. The total flame is therefore sufficiently energetic to assure a successful ignition whenever the runaway exothermic processes at the propellant surface are triggered. Accordingly, self-sustaining ignition is predictable by a simple thermal theory which is capable of predicting surface temperature at ignition.

The IR signal thresholds obtained with a noncatalyzed DB propellant (Fig. 13) and a catalyzed DB propellant (Fig. 14) indicate the extent that atmospheric oxygen and increased pressure accelerate the reactions near the propellant surface. The important features are: (1) as indicated on Figs. 13 and 14, the appearance of the faint surface region reactions (L_{1b}) depends neither on the pressure level nor on the nature of the pressurizing gas; (2) as shown on Fig. 13, the development in time of strong surface region reactions depends both on the pressure level and on the nature of the pressurizing gas; (3) the appearance of the faint surface region reaction (L_{1b}) is nearly coincident with the separation line between ignition and no ignition regions (L_{1d}) in air (see Figs. 16 and 13) and in N_2 at the high pressure region (see Figs. 6 and 11).

D. Effect of Radiation Source

The results obtained with noncatalyzed DB propellants containing different amounts of carbon powder evaluated in the arc image ignition apparatus (Fig. 15) show L_{1d} limit (i.e., self-sustaining ignition) pressure sensitivities not obtained in the laser ignition apparatus (Figs. 6 and 12). Thus the magnitude of the pressure sensitivity is a function of the apparatus.

The behavior of nonmetallized AP composite propellants is similar in the laser and arc image ignition apparatus (see Fig. 4), in that no pressure dependence is found, but the radiative heating of the solid phase is markedly different, due to the different reflection, absorption, and scattering in depth of the radiant energy. Note that the ignition boundaries are all essentially parallel. Neither the addition of 1% carbon (propellant 2) nor the simultaneous change of AP particle granularity and mixture ratio (propellant 3) affect the ignitability of the AP composite propellants in the laser apparatus.

The ignition characteristics of catalyzed DB propellants are very similar in the laser and arc image ignition apparatus (see Fig. 5). The L_1 limit is achieved faster with the laser indicating that more of the laser radiation is concentrated at the propellant surface. The dynamic extinction of noncatalyzed propellants (the L_2 limit) observed in the laser ignition tests do not occur in the arc image test (compare Figs. 6 and 12 with Fig. 15).

E. Effect of Carbon Powder

All of the unmodified propellants transmit a large faction of the incident panchromatic (0.2 to 1.6μ) radiation from the xenon lamp but are relatively opaque to the 10.6μ radiation of the laser. From all indications, both the composite propellants and the DB propellants concentrate the laser radiation at their surfaces and the addition of carbon has no effect on laser ignition times. This can be seen by contrasting laser and arc image data on Fig. 4 and by contrasting the laser data of Figs. 6 and 12 with the arc image data of Fig. 15. The laser radiation ignites the materials in 1/10th of the time required by xenon lamp. To quantify the effects of reflection and penetration of radiation, propellants 7 and 8, with 0.2 and 1.0% submicron carbon powder respectively, were tested. Arc image ignition tests of propellant 8 with 1.0% carbon powder produced ignition times comparable to the ignition times obtained using the laser. This suggested that the small amount of carbon opacifies the propellant in the 0.2 to 1.6μ range. The Ballistics Research Laboratories measured reflectivity and absorptivity of the propellants over the wavelength region from 0.2 to 2.0μ (see Table III). In all cases, the 0.2% carbon effectively reduces the reflectivity to zero. However, the in-depth extinction coefficient is very dependent on wavelength and carbon percentage.

A transient heat conduction formulation with wavelength-dependent radiation penetration in depth was solved to study the influence of radiation penetration on ignition time. Particular attention was given to the difference between the extinction coefficient and the absorption coefficient. The solution is being used to define conditions under which in-depth penetration of radiation dominates the ignition delay.

V. DYNAMIC RESPONSE TO RAPID DERADIATION

A. Experimental Results

The experimental situation in which double base propellants are subjected to varied radiant heat fluxes provides a controlled method of creating transient flames of either increasing or diminishing intensity. The results, in addition to providing insights into the nature of propellant flammability limits, permit testing of flame theories and, further, have broad implications in the continuing search for a quantitative measure of the susceptibility of propellants to various forms of combustion instability. The companion analytical studies have yielded a mathematical model that successfully correlates many of the observed trends.

Extensive tests of this nature in which propellants have been subjected to varied radiant pulses show that noncatalyzed double base propellant compositions exhibit an apparently paradoxical behavior. The flux-time domain of ignitability has, in addition to the usual lower bound (i.e., the L_{1d} limit), an upper bound (i.e., the L_2 limit) above which irradiation leading to flame development is invariably followed by extinction, not steady burning. The existence of the L_2 limit implies that too much ignition stimulus yields no ignition just as does too

little stimulus. This unexpected behavior has thus far been observed with five quite normal double base formulations, propellants 5, 6, 7, 8 and a plastisol NC/NG (see Table I in Ref. 2). This behavior is not seen in nitrate ester propellants containing platonizing catalysts (lead or copper salts).

Diagnostic tests indicate that L_2 limits are due to dynamic instability brought on by rapid removal of the ignition stimulus (referred to as deradiation; one must distinguish between the time at which deradiation begins and the interval of time which it requires). The effect is quite analogous to depressurization extinction; in both cases, an externally imposed rapid disturbance upsets the balance of energy fluxes at the propellant surface to such a degree that the surface temperature and hence the burning rate decay drastically and extinction ensues.

Evidence for this dynamic character of the L_2 limit comes from several types of results. High speed shadowgraph movies (as well as thermocouple and IR detector results) clearly show that gaseous flame development begins at approximately the time the minimum (lower) ignition boundary is crossed. The flame continues to develop and persists even when the irradiation crosses the upper ignition boundary; however, as soon as (and only when) the radiant flux is terminated, extinction of the flame follows. Figure 9 shows several frames from a high speed shadowgraph movie which illustrate this sequence of events.

The hypothesis implies that lessening the perturbation severity or stabilizing the flame should push the L_2 limit upward (broaden the ignitable domain). These implications of the proposed mechanism were verified experimentally; the results are shown in Fig. 2 and Fig. 3 of Ref. 2. Increased pressure stabilizes the flame in two ways, first, it increases the conductive heat fluxes in the surface region thereby making the external radiant flux relatively smaller (and its removal less disturbing); second, increased pressure increases the propellant burning rate and thereby decreases the propellant relaxation time (making it smaller relative to the flux removal time). For propellant 5, the broadening of the ignitable domain is substantial when the pressure is increased from 10 atm to 20 atm; when the pressure is further increased to 34 atm, the upper ignition bound disappears completely for the range of fluxes and times shown in Fig. 2 of Ref. 2.

Increasing the deradiation interval (time to decrease the radiant flux from its maximum value to zero) represents a lessening of the perturbation severity because it allows the propellant more time to adjust its temperature profile while the radiant flux is being removed. Figure 3 of Ref. 2 illustrates the experimentally observed effect of increased deradiation interval on the extent of the ignitable domain for M-9 at a fixed pressure. The deradiation intervals given are the total times to terminate the flux. As predicted, increasing the deradiation interval from 1 to 2 msec increases the extent of the ignitable domain by raising the upper ignition boundary; the L_2 limit disappears when the deradiation interval is increased to 10 msec.

Further evidence for the dynamic character of the extinction phenomenon comes from steady burning experiments. Propellants were ignited with a hot wire and allowed to achieve a steady burning condition. They were then subjected to a radiant pulse of fixed time of termination (2 msec), but variable intensity and duration. The final effect of the disturbance associated with this external energy stimulus (i.e., continuation of combustion or extinction) was recorded. Three different propellants were tested: two non-platonized compositions (propellant 5 and a similar NC/NG plastisol composition) and one platonized (propellant 9).

The range of pressures examined goes from 1 to 10 atm. The results obtained are shown in Fig. 17; the minimum duration pulse required to extinguish a steadily burning sample is plotted versus intensity of the radiant flux. In the range of parameters examined, the catalyzed propellant could not be extinguished by a radiation pulse. Note that for a fixed intensity of the pulse, the minimum duration of the pulse required for extinction (when it occurs) increases as the pressure increases (see propellant 5 at 6.8 and 10 atm).

We explored those chemical-physical changes that either eliminate the L_2 limit or increase the ignition domain, i.e., (1) using arc image rather than laser radiation (compare Fig. 15 with Figs. 6 and 12), (2) adding catalysts (compare propellant 10 of Fig. 11 with propellant 7 of Fig. 12), (3) adding relatively large amounts of carbon powder (Fig. 12), (4) replacing N_2 with air (Fig. 16), (5) very long deradiation times (Fig. 3 of Ref. 2), and (6) increasing pressure (21 versus 11 atm for propellant 6 on Fig. 6 and for propellant 5 of Fig. 3 in Ref.2).

Figure 12 illustrates the importance of understanding the conditions that produce an L_3 boundary. Tests of propellant 8 with 1.0% carbon at 11 atm produced a boundary between the no-ignition and ignition regions that on first examination appears to be a L_{1d} limit with a very peculiar slope. However, once it is realized that the limit is a L_3 limit, it becomes apparent that decreasing the test pressure decreases the width of the ignition corridor between the L_{1d} and L_2 limits (see Fig. 2 of Ref. 2). Indeed, at 11 atm the L_{1d} and L_2 limits merge and the ignition corridor does not exist.

Comparison with Figs. 6 and 12 shows that the addition of 0.2 carbon (propellant 7) has no sensible influence on the L_2 and L_3 limits, whereas the addition of 1% C (propellant 8) has a profound influence on the dynamic response (especially the L_3 limits). The ignition corridor at 21 atm is reduced by the addition of 1% C and completely eliminated at 11 atm. Apparently, the added carbon somehow accelerates the previously described flame spreading away from the target area.

As indicated on Fig. 6, the dynamic extinction pressure dependence of propellant 6 is accentuated in such a way that at 11 atm the L_2 limit (which exists for propellant 5[2]) merges with the L_{1d} limit and the ignition corridor is completely wiped out.

B. Flame Theory Interpretation

To obtain an understanding of how compositional changes can lead to the instabilities associated with dynamic extinction, the kinetics and the energetics at the surface and in the gas phase must be considered. Unfortunately, for DB propellants only approximate information is available on the reactions and on the relative proportions of the heat of combustion liberated in the surface reaction layer and in the closely adjacent region of the gas phase flame. In what follows, we necessarily resort to speculation. The energy feedback to the condensed phase, q_{fb}, may be considered in two parts

$$q_{fb} = q_s + q_f \tag{1}$$

where q_s is the contribution within the surface reaction layer and q_f is the heat feedback from the gas phase. Previous studies[17,19,20] explained that the approximate function dependencies of q_s and q_f with burning rate are

$$q_s \sim Q_s r \quad \text{and} \quad q_f \sim f(p)/r \tag{2),(3)}$$

where Q_s is the heat released at the surface per unit volume. Equa-

tion (3) was developed for the small perturbations associated with intrinsic stability analyses. However, it has been shown[19] that its simple form is useful when considering the larger forced perturbations, such as those caused by rapid deradiation and rapid pressure changes. Experiment and theory have shown that formulation changes that increase q_s with respect to q_{fb} increase the sensitivity to instability (and thus, dynamic extinction). For convenience, a parameter H is defined as q_s/q_{fb}. The statements in Refs. 19 and 21 that lowering the value of H tends to stabilize the burning rate against a disturbance is explained by the inverse dependence of q_f on r, which tends to oppose any disturbance that changes r. Conversely, the proportional dependence of q_s on r tends to reinforce disturbances that change r. It has been shown[16] that adding Pb and Cu salts to DB propellants increases the burning rate by increasing the heat feedback from the flame zone rather than by increasing Q_s at the surface, i.e., H is lower than for the noncatalyzed DB propellants. The data clearly indicate that catalyzed DB propellants do not experience dynamic extinction (Figs. 5 and 11) and that noncatalyzed DB propellants do (Figs. 6 and 12). Thus there is consistency between the studies that explain the effects of catalysts and the studies that explain dynamic extinction.

Another contributing factor is that the thermal inertia of the carbonaceous layer on the catalyzed DB propellants acts to damp the rapid changes in the flame zone that are required for dynamic extinction.

The fact that AP composite propellants do not experience dynamic extinction by deradiation (at least at the pressures and deradiation times considered in this paper) is also explained by their relatively low H values, as compared to what are believed to be the higher H values of noncatalyzed DB propellants. An approximate ranking of H can be obtained without directly measuring q_f or q_s from one of the analytical expressions for temperature sensitivity of burning rate,[21] σ_p,

$$\sigma_p \sim [2(T_s - T_0)(1 - H)]^{-1} \qquad (4)$$

which shows that increased values of H correspond to increased values of σ_p. Indeed, the σ_p values of noncatalyzed DB propellants are generally twice as high as the σ_p values for composite propellants. Consistent with the theories, the noncatalyzed DB propellants are easily extinguished (both by depressurization[20] and deradiation[2]) and should have relatively high H values. Also, the σ_p values of PbSa and CuSa catalyzed DB propellants tend to be lower than those of noncatalyzed propellants.[16,22]

VI. PRECAUTIONARY ASPECTS OF RADIATION EXPERIMENTS

Ignition boundaries obtained with radiative apparatus differ from those obtained using other ignition sources. Indeed, in this study we are using these differences to elucidate the processes that occur during ignition.

The distorting effects of solid propellant transparency have been shown clearly by the addition of small amounts of finely dispersed carbon black to AP composite and double base propellants (see Figs. 4 and 15).

The slow chemical kinetics in the cool gas phase near the surface during radiative ignition may produce results that are contradictory to the conductive ignition results obtained by end-wall testing in shock tubes. For one thing, ignition times in radiative ignition tests are much longer than in equivalent convective or conductive tests. This was demonstrated by comparative testing of propellants 5 and 9 by the laser

and by end-wall shock tube using air as the driven gas. In the laser, radiative ignition of propellant 9 is possible in a low pressure range where propellant 5 is not ignitable. Conversely, in the end-wall shock tube under 60 atm test conditions, conductive ignition of propellant 5 (at high pressure, at least) requires a heating time of approximately 3 msec while propellant 9 requires a heating time greater than 15 msec which is much longer than the time of expansion wave return.

A comparison of radiative ignition with ignition by convective heating (from hot combustion gases flowing parallel to the propellant surface) was shown in Ref. 23. In general, the convective ignition requires significantly less energy than radiative ignition. Aluminum as a fuel additive decreases the energy required for radiation ignition by concentrating near the propellant surface the effects of radiant heating. In the case of convective heating, aluminum increases the energy required for ignition; this increase is expected as a result of increased propellant thermal conductivity.

The combustion dynamics leading to possible extinction during the deradiation interval may alter the location of the L_{1d} boundary in go/no-go testing of a propellant under radiation by creating an artificial nonignition region. In Figs. 6 and 12, this is demonstrated for a noncatalyzed DB propellant; it may occur for other propellants depending on the pressure and deradiation interval. This is a unique consequence of radiative stimuli, since the abrupt termination of heating required for dynamic extinguishment is improbable using either conductive or convective sources.

The spatial distribution of the impinging radiation on the target surface involves 3-dimensional heating effects at the edges which may influence the ignitability of propellants examined either by arc image or laser. For example, the dynamic extinction boundary is not observed in arc image tests for any of the propellants since the weaker heat flux surrounding the target spot provides a region where the flame is less sensitive to the disruption in the energy balance necessary for deradiation extinction. Also, the spatial structure of a radiation beam is never uniform and therefore gasification and development of the flame are triggered nonuniformly on the sample surface. For a laser with an interface pattern (resulting from the laser beam interacting with the mirror and kaleidoscope), hot spots can be significant. The successive spreading of the flamelets (Fig. 8) also depends on the structure of the laser beam. In the case of AP composite propellants, the nonhomogeneous matrix of the sample may further affect the local ignition behavior of the propellant when subjected to radiant heating.

VII. ANALYTICAL MODEL OF TRANSIENT RESPONSES DURING IGNITION SEQUENCE

A properly posed analytical model must account for the interdependence of the heat feedback from the flame on burning rate. A flame model for solid propellant combustion could have been used. However, the key parameters (in even the simplest global formulations) such as the gas phase activation energy, reaction order, and fraction of heat release that occurs on the surface are only crude approximations. In our analytical development, we started with basic premises of Zeldovich[24] since this method offers important advantages when considering the burning rate transients of propellants for which the details of the reaction mechanisms have not been established. The method starts with measured steady-state burning rate data and pyrolysis data as functions of pressure and ambient temperature and deduces a heat feedback function from the gas to the solid in the proper form for application to nonsteady burning situations.

The important assumptions are:

1. The rate processes in the gas phase and in the surface reaction zone can be considered quasi-steady in the sense that their characteristic times are short compared to condensed phase characteristic times.
2. No kinetic heat release occurs in the condensed phase below the surface reaction zone. Although the surface reactions occur in a zone of finite thickness, the zone is sufficiently thin that it can be considered as quasi-steady.
3. The propellant is homogeneous and isotropic.

The justifications for the assumptions follow Ref. 21. Assumption one is valid for our conditions as can be shown by comparing the magnitude of the characteristic times (e.g., at typical noncatalyzed NC composition at 10 atm):

$$\text{condensed phase,} \quad \tau_c = \alpha_c/r^2 = 0.020 \text{ sec} \tag{5}$$

$$\text{surface,} \quad \tau_s \sim (RT_{if}/E)\tau_c < 0.002 \text{ sec} \tag{6}$$

$$\text{flame zone,} \quad \tau_f = [\lambda_f c_c \rho_f/(\lambda_c c_f \rho_c)]\tau_c \sim 0.01\tau_c < 0.0001 \text{ sec} \tag{7}$$

Accordingly, τ_s and τ_f are small compared to τ_c and the heating times.

The energy equation in the condensed phase ($-\infty<x\leq 0$) has the following eigenvalue dependence on $\phi(0,t) = \phi_{if}(t)$

$$\rho_c c_c[\partial T/\partial t + r\phi] = \lambda(\partial\phi/\partial x) \tag{8}$$

The initial condition is $T(x,0) = T_0$ (9)

The first boundary condition is $\partial T/\partial x \to 0$ as $x \to -\infty$ (10)

The second boundary condition is a series of sequential conditions:

1) heatup to gasification

$$\lambda_c(\partial T/\partial x)_{c,if} = q(t) \quad \text{for} \quad 0^+ < t \leq t_v \tag{11}$$

2) gasification prior to establishment of flame

$$= q(t) - r\rho_c\Delta h \quad \text{for} \quad t_v < t \leq t_f \tag{12}$$

3) combined heating from ignition stimulus and from flame zone reactions

$$= q(t) + \lambda_c\phi_{if}(r,p) \text{ for } t_f < t \leq t_{off} \tag{13}$$

where $q(t)$ varies in a prescribed manner, e.g., a linear decrease from maximum q to zero in 0.001 sec corresponding to the deradiation interval.

4) adiabatic combustion without external stimulus

$$= \lambda_c\phi_{if}(r,p) \quad \text{for} \quad t > t_{off} \tag{14}$$

5) optionally, after steady state burning is achieved, an externally imposed heat flux as an arbitrary function of time, e.g., a pulse.

The nonsteady heat feedback function, ϕ_{if}, is developed in Ref. 21 except that it is based on T_{if} rather than a so-called burning-surface temperature (i.e., the temperature at the gas/burning surface interface). Once it is realized that in the case of double base propellants the surface temperature observations are complicated by items such as filigree, carbonaceous residues glowing in the flame zone, it is more meaningful to use a T_{if} which corresponds to the interface between the zone of important exothermic reactions and the nonreacting condensed phase. As explained in Ref. 21, the nonsteady heat feedback function, ϕ, is deduced from measured burning rates as functions of pressure and initial temperature.

Equation 8 along with its conditions, Eqs. 9 - 14, were solved using the methods of explicit finite differences. The model was used to generate several series of calculated results that simulated the laser ignition experiments. The calculations were carried out using the properties of the NC/NG composition listed in Table II of Ref. 2. We selected this propellant because its combustion characteristics, particularly $r(p,T_0)$, have been evaluated most thoroughly in the range of interest.[22] Figure 18 shows burning rate versus time histories for situations where deradiation begins (1) before the requirements for sustained ignition are achieved; (2) during the interval which sustained ignition will result; and (3) after the propellant has been driven to the point that deradiation results in extinguishment; the correspondence of this behavior with that found experimentally is evident. Note that increasing the deradiation interval from 0.001 to 0.003 sec softens the perturbation caused by deradiation and, thereby, extends the interval of ignition. Similar calculations were performed for situations corresponding to propellant 9 where the combustion characteristics decrease the tendency for deradiation extinguishment. By repeating the calculations in a go/no-go fashion, calculated combustion limits (with pressure as a parameter) are found which agree with the observed trends for N-5 as shown in Fig. 11. By using the mathematical model to also simulate the pulse experiments, we have demonstrated extinctions similar to those of Fig. 11. Generally, the laser pulse must be of sufficient duration that the preheated region corresponding to the slower burning rate prior to the pulse has been burned away.

VIII. IGNITION OF SINGLE CRYSTALS

The ignition and transient combustion of HMX crystals, AP crystals, NC propellants, and AP composite propellants are being studied using results from high speed (5000 frames/sec) shadowgraphs and color movies. The ignition source is the laser. The tests are carried out in N_2 and CH_4. The CH_4 atmosphere is used to promote gas phase reactions between the decomposition vapors (e.g., HMX and AP) and the surrounding gases. The film sequences illustrate that three of the systems differ greatly: (1) the AP monopropellant flame is relatively cool (1200-1400°K) and reacts with surrounding fuel vapors to produce an intense flame close to the surface; (2) HMX burns as a monopropellant with a very hot flame (>3000°K) and its nearly balanced flame is cooled by interactions with fuel vapors; and (3) NC burns with a moderately hot flame that is several mm from the surface and undergoes a small temperature change when it interacts with other ingredients.

The films indicate that HMX crystals fracture during rapid ignition. This fracture is important evidence that supports the theory that thermal stress contributes to the exponent shift of HMX composite propellants.

The nearly parallel plumes from AP surface indicate that AP gas phase reactions are completed at the surface. Expansion of gas above the HMX crystal indicates that a large portion of the HMX gas phase reactions occur above the surface. Ignition of HMX and AP is not accelerated by replacing N_2 with CH_4 (at 21 atm and 67 cal/sec-cm^2). Highly loaded AP composite propellants exhibit ignition delays comparable to neat AP, but their flame development times are relatively short.

IX. CONCLUSIONS

The ignition trends of different propellant types (e.g., AP composite vs double base) and of several modified propellants (e.g., noncatalyzed vs catalyzed double base and transparent vs opaque propellants) have been rationaized in terms of basic differences in the structure of the deflagration wave in the solid and gas phases. In addition, for each propellant the data clearly isolate the domains (pressure, ignition stimulus, and propellant type) where simple thermal theories fail and those domains where theories taking into account the interaction of the incipient gas phase with the solid phase are required.

The ignition boundaries obtained with radiative ignition apparatus differ from those obtained using other energy sources. However, radiative ignition tests are very valuable because they permit a relatively uncomplicated diagnosis of combustion properties.

Compared to the arc image, using the laser greatly reduces the shortcomings of radiation ignition experiments since (1) reflectivities at 10.6μ are relatively low, (2) absorbtivities at 10.6μ are relatively high, and (3) the parallel beam reduces questions about effects of incidence angle.

The observed ignition processes and ignitability limits have been explained and correlated by the mathematical model which is an extension of the approach taken by Zeldovich. The significance of these studies goes beyond an explanation of observed ignition and extinguishment limits. By developing the capability of correlating the trends observed in the relatively uncomplicated go/no-go ignition test, the analytical method simultaneously qualifies as being suitable for considering more complex practical situations that involve nonuniform heating, transient pressure fields, complex geometrics, etc.

REFERENCES

1. DeLuca, L., Caveny, L. H., Summerfield, M., "A Comparative Study of Radiative Ignition Characteristics of Solid Propellant," to appear in AIAA Journal.

2. Ohlemiller, T. J., Caveny, L. H., DeLuca, L., and Summerfield, M., "Dynamic Effects on Ignitability Limits of Solid Propellants Subjected to Radiative Heating," Fourteenth Symposium (International) on Combustion, The Combustion Institute, 1973, pp. 1297-1307.

3. Price, E. W., Bradley, H. H., Jr., and Hightower, J. D., and Fleming, R. O., Jr., "Ignition of Solid Propellants," AIAA preprint No. 64-120, 1964.

4. Lenchitz, C., Hayes, E., Velicky, R. W., and Silvestro, G., "The Ignition Characteristics of Nitrocellulose," First Review of AMC-Fundamentals of Ignition Task-BRL, Aberdeen Proving Ground, Md., 1971.

5. Hicks, B. L., "Theory of Ignition Considered as a Thermal Reaction," J. Chem.Phys., Vol. 22, Pt. 1, No. 3, 1954, pp. 414-429.

6. McAlevy, R. F. III, Cowan, P. L., and Summerfield, M., "The Mechanism of Ignition of Composite Solid Propellants by Hot Gases," ARS Progress in Astronautics and Rocketry: Solid Propellant Rocket Research, Vol. 1, edited by M. Summerfield, Academic Press, New York, 1960. pp. 623-652.

7. Hermance, C. E., Shinnar, R., and Summerfield, M., "Ignition of an Evaporating Fuel in a Hot Oxidizing Gas Including the Effect of Heat Feedback," Astronautica Acta, Vol. 12, No. 2, 1966, pp. 95-112.

8. Waldman, C. H. and Summerfield, M., "Theory of Propellant Ignition by Heterogeneous Reaction," AIAA Journal, Vol. 7, No. 7, July 1969, pp. 1359-1361.

9. Bradley, H. H. and Williams, F. A., "Theory of Radiant and Hypergolic Ignition of Solid Propellants," Combustion Science and Technology, Vol. 2, No. 1, August 1970, pp. 41-52.

10. Hermance, C. E. and Kumar, R. K., "Gas Phase Ignition Theory for Homogeneous Propellants under Shock Tube Conditions," AIAA Journal, Vol. 8, No. 9, September 1970, pp. 1551-1558.

11. Koval'skii, A. A., Khlevnoi, S. S., and Mikheev, V. F., "The Ignition of Ballistite Powders," Combustion, Explosion, and Shock Waves, Vol. 3, No. 4, 1967, pp. 527-541.

12. Librovich, V. B., "Ignition of Powders and Explosives," Zhurnal Prikladnoi Mekhaniki i Technicheskoi Fiziki, No. 6, Nov-Dec 1963, pp. 74-80.

13. Anderson,W. H., "Theory of Surface Ignition with Application to Cellulose, Explosives and Propellants," Combustion Science and Technology, Vol. 2, 1970, pp. 213-221.

14. Price, E. W., Bradley, H. H., Jr., Dehority, G. L., and Ibiricu, M. J., "Theory of Ignition of Solid Propellants," AIAA Journal, Vol. 4, No. 7, July 1966, pp. 1153-1181.

15. Ohlemiller, T. J. and Summerfield, M., "Radiative Ignition of Polymeric Materials in Oxygen/Nitrogen Mixtures," Thirteenth Symposium (International) on Combustion, The Combustion Institute, 1971, pp. 1087-1094. Also AMS Report 876, Princeton University, Princeton, N. J., August 1969.

16. Kubota, N., Ohlemiller, T. J., Caveny, L. H., and Summerfield, M., "The Mechanism of Super-Rate Burning of Catalyzed Double Base Propellants," AMS Report No. 1087, March 1973, Princeton University, Princeton, N.J. (AD 763 786)

17. Steinz, J. A., Stang, P. L., and Summerfield, M., "The Burning Mechanism of Ammonium Perchlorate-Based Composite Solid Propellants," AIAA Paper 68-658, June 1968; also AMS Report No. 830, February 1969, Princeton University, Princeton, N.J. (AD 688 944)

18. Derr, R. L., Beckstead, M. W., and Cohen, N. S., "Combustion Tailoring Criteria for Solid Propellant," Lockheed Propulsion Company Report No. 835-F, Technical Report AFRPL-TR-69-190, May 1969.

19. Krier, H., T'ien, J. S., Sirignano, W. A., and Summerfield, M., "Nonsteady Burning Phenomena of Solid Propellants: Theory and Experiments," AIAA Journal, Vol. 5, No. 2, Feb. 1968, pp. 178-185.

20. Merkle, C. L., Turk, S. L., and Summerfield, M., "Extinguishment of Solid Propellants by Depressurization: Effects of Propellant Parameters," AIAA Paper No. 69-176, New York, Jan. 1969; also AMS Report No. 880, Princeton University, Princeton, N.J., July 1969. (AD 697 661)

21. Summerfield, M., Caveny, L. H., Battistia, R. A., Kubota, N., Gostintsev, Yu. A., and Isoda, H., "Theory of Dynamic Extinguishment of Solid Propellant with Special Reference to Non-Steady Heat Feedback Law," Journal of Spacecraft and Rockets, Vol. 8, No. 3, March 1971, pp. 251-258.

22. Kubota, N., Caveny, L. H., and Summerfield, M., "Temperature Sensitivity of Double-Base Propellants," Proceedings of 1971 JANNAF Combustion Meeting, CPIA Publication 220, Nov. 1971, pp. 387-401.

23. Ohlemiller, T. J., and Summerfield, M., "A Critical Analysis of Arc Image Ignition of Solid Propellants," AIAA Journal, Vol. 6, No. 5, May 1968, pp. 878-886.

24. Zeldovich, Ya. B., "On a Burning Rate under Nonsteady Pressure," Zhurnal Prikladnoi Mekhaniki i Technicheskoi Fiziki, No. 3, January-February 1964, pp. 126-130.

NOMENCLATURE

c	Specific heat, cal/g°K
E	Activation energy in pyrolysis law, cal/g-mole
H	Ratio of heat feedback from surface reactions to total heat feedback
I_0	Incident radiant flux intensity, cal/cm^2-sec
p	Pressure, atm
q	Radiative ignition stimulus, cal/cm^2-sec
Q_s	Heat released at the burning surface, cal/cm^3
r	Burning rate, cm/sec
R	Universal gas constant, 1.98, cal/g-mole°K
t	Time, sec
T	Temperature, °K
x	Distance, cm
α	Thermal diffusivity, cm^2/sec
β	Radiation extinction coefficient, cm^{-1}
Δh	Heat of gasification before flame formation, cal/g
λ	Thermal conductivity, cal/cm-°K-sec
ρ	Density, g/cm^3
σ_p	Temperature sensitivity of burning rate at constant pressure $(\partial \ln r/\partial T_0)_p$, °K
τ	Characteristic time, sec
ϕ	Temperature gradient in condensed phase, °K/cm
~	Value is on the order of

Subscripts

0	Ambient conditions
c	Condensed phase
eq	Steady state condition
f	Flame zone
fb	Feedback to propellant
if	Interface between the very thin surface reaction zone and and nonreacting condensed phase
off	Radiant flux removed
s	Surface reaction zone
v	Surface gasification before flame

Table I Propellants used in ignition experiments[a]

Ammonium perchlorate (AP)/hydrocarbon binder composite propellants:

Nonmetallized -

1. 75% AP (45μ) without C (Batch 1086)
2. Same as 1 but with 1% C (Batch 1087)
3. 80% AP (30% 15μ and 70% 180μ) (Batch 1020)

Metallized -

4. 24% AP and 51% boron

Nitrocellulose (NC) double base (DB) propellants:

5. Standard U.S. Army M-9 (39.6% NC, 49.4% NG, 11.0% plasticizer and stabilizer)
6. Nitrocellulose (NC) Plastisol (53.7% NC, 39.2% trimethylolethane trinitrate (MTN), 7.1% triethylene glycol dinitrate (TEGDN)) (Batches 1069 and 1970)
7. Opacified NC plastisol, No. 6 with 0.2% C (Batch 1059)
8. Opacified NC plastisol, No. 6 with 1.0% C (Batch 1088)
9. Standard U.S. Navy N-5 (50.0% NC, 34.9% NG, 12.5% plasticizer and stabilizer, 2.6% Pb salts) (A JANNAF reference propellant)
10. Catalyzed NC plastisol, No. 6 with 2.0% lead salicylate (PbSa) and copper salicylate (CuSa) and 0.2% C (Batch 1050)

Nitramine (HMX)/polyurethane (PU) propellants:

11. High energy propellant (85% HMX, 15% PU)
12. Cool propellant (75% HMX, 15% PU, 10% oxamide)
13. Propellant No. 11 containing 0.4% elemental phosphorus in the form of ammonium polyphosphate.

[a] Propellants 1, 2, and 3 were processed at Princeton using standard techniques.[17] Propellant 4 was supplied by the Huntsville Division of the Thiokol Chemical Corporation. Propellants 6, 7, 8, and 10 were processed at Princeton using the techniques described in Ref. 22. Propellants 11, 12, and 13 were supplied by the Wasatch Division of the Thiokol Chemical Corporation. Propellants 9 and 10 were catalyzed to produce increased burning rates and plateaus between 10 and 80 atm. Carbon was added to propellants 2, 7, 8, and 10 in the form of a powder (Neo Spectra TA, manufactured by Columbian Carbon Co.) with a mean diameter on the order of 0.01μ.

Table II

Scope of tests described in paper[a]

Propellant Number	Pressures used in Arc Image Tests, atm. N_2 5	N_2 11	N_2 21	Air 5	Air 11	Air 21	Pressures used in Laser Tests, atm N_2 5	N_2 11	N_2 21	Air 5	Air 11	Air 21	Deradiation Extinction Boundary Established	Pressure Flux (cal/sec-cm^2)
1	4	4	4				4	4	4				No	11 atm N_2; 30
2	4	4	3, 4				4	4	4				No	
3							4	4	4				-	
4		4	3, 4										-	
5								T	6				Yes	21 atm N_2; 51
6	15	15	3, 15					13	13	13, 16	13, 16	13, 16	Yes	
7	15	15	3, 15					T	12	16	16	16	Yes	
8	15	15	3, 15					12	12	16	16	16	Yes	
9	11	11	11				11	11	11				No	4 atm N_2; 42
10	5	5	3, 5				5, 11, 14,	5, 11, 14	5, 11, 14	14, 16	14, 16	14, 16	No	
11	T	7	7				T	T	T	T			-	
12		T		7	7	7	T	T	T	T			-	
13	T	T	3,7						T	T			-	

[a]Numbers refer to figure in which data appears. The entry T means that data are discussed only in the text.

Table III Reflectivities and extinction coefficients of the propellants at the 10.6μ wavelength of the CO_2 laser.

	r_e @10.6μ	r_e @0.9μ	$\bar{r}_e$ 0.2 to 2.0μ	β CM^{-1} @10.6
○ AP/HYDROCARBON BINDER COMPOSITE PROPELLANTS:				
1. 75% AP (45μ) WITHOUT C	0.013	0.40	0.01	---
2. SAME AS 1 BUT WITH 1% C	0.038	0.05	0.04	---
○ DOUBLE BASE PROPELLANTS:				
6. NC PLASTISOL (53.7% NC, 39.2% MTN, 7.1% TEGDN)	0.003	0.70	0.59	950
7. OPACIFIED NC PLASTISOL, No. 6 with 0.2% C	0.026	0.055	0.06	1500
8. OPACIFIED NC PLASTISOL, NO. 6 WITH 1.0% C	0.016	0.050	0.05	1900
10. CATALYZED NC PLASTISOL, NO. 6 WITH 2.0% Pb and Cu SALTS, 0.2% C	0.025	0.060	0.06	1900
○ HMX/POLYURETHANE (PU)				
11. 85% HMX, 15% PU	0.063	0.86	0.81	---
12. 75% HMX, 15% PU, 10% OXAMIDE	0.033	0.41	0.40	---

*From data of I. W. May and R. Wires at BRL.

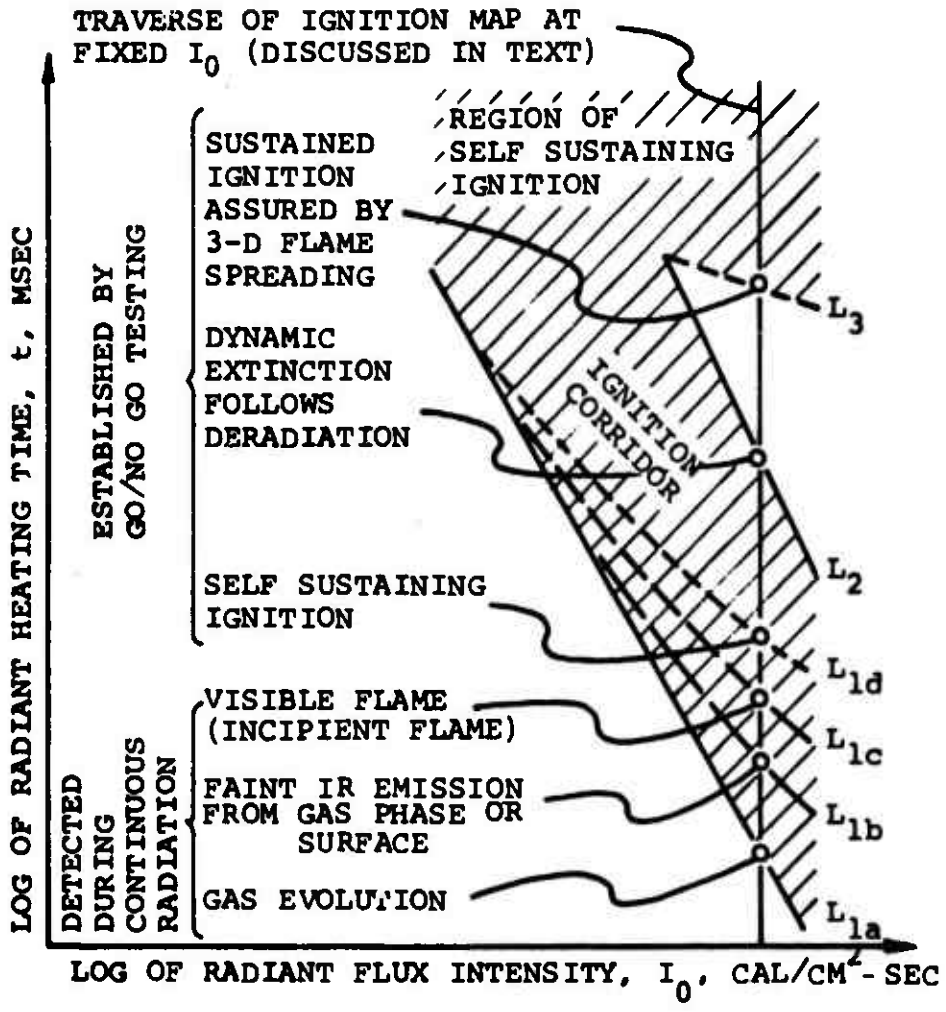

Fig. 1 Generalized ignition map showing event limits or signals that occur during radiant heating of solid propellants.

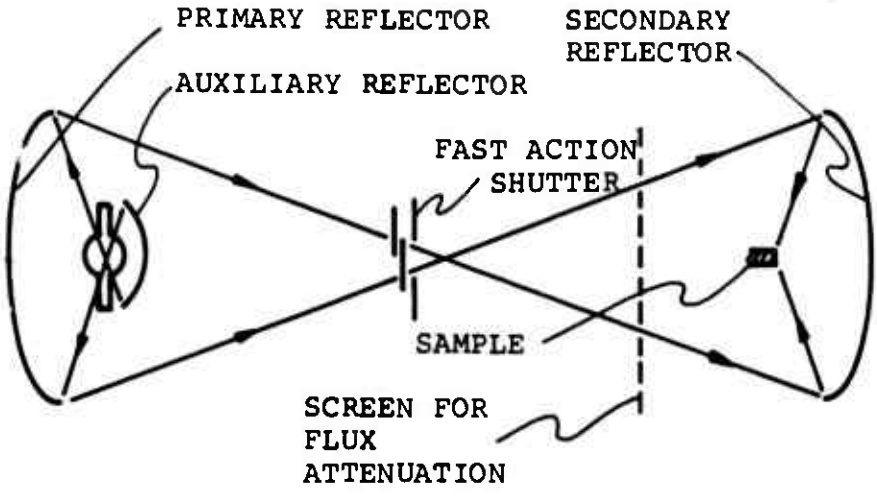

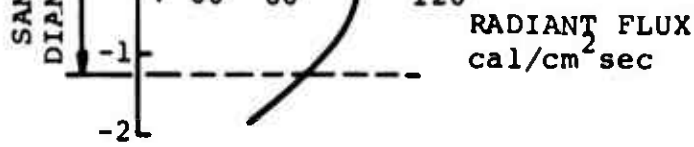

TYPICAL ILLUMINATION PROFILE ON SAMPLE

Fig. 2a Schematic diagram of arc image ignition apparatus.

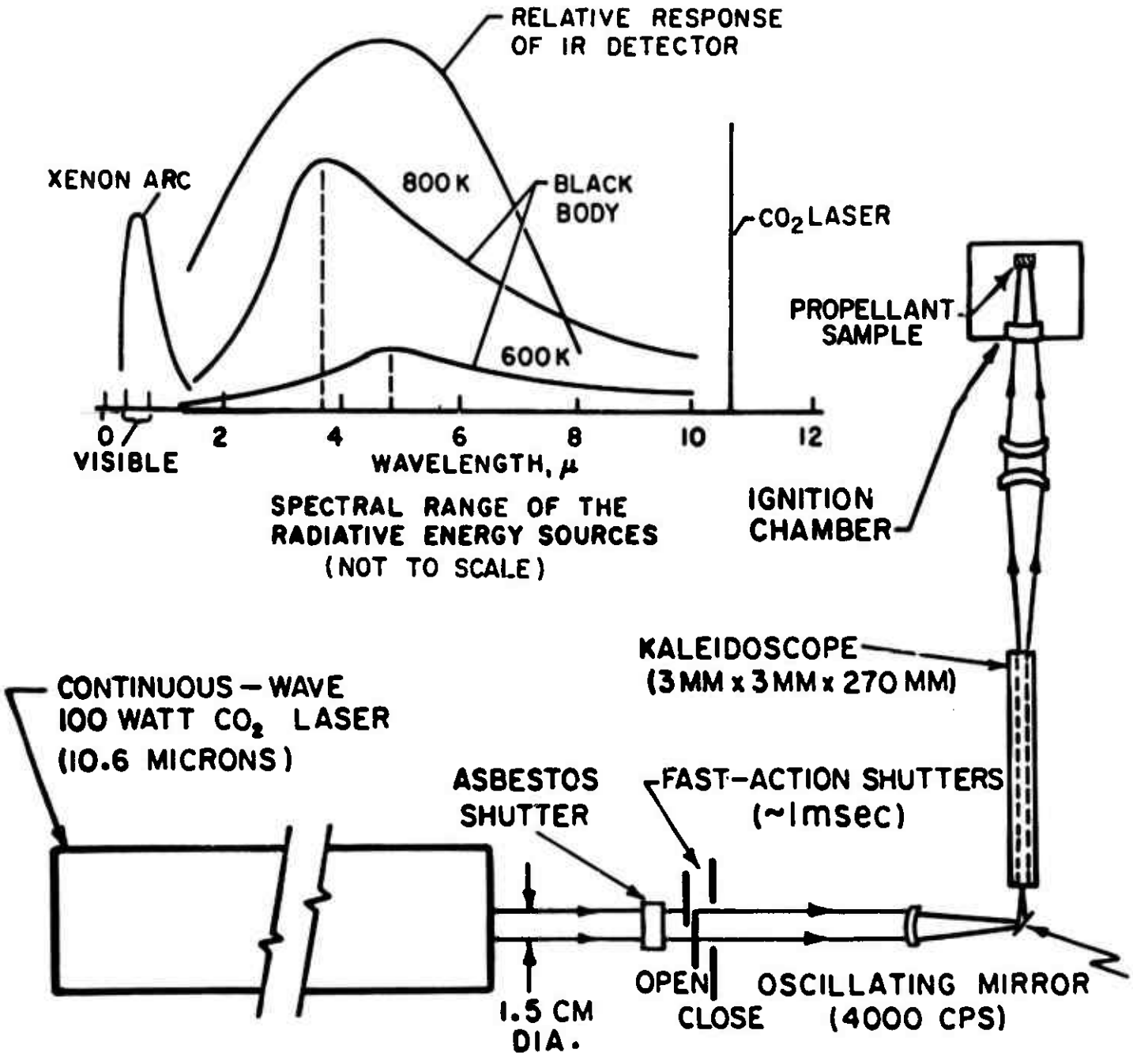

Fig. 2b Schematic diagram of laser ignition apparatus showing spectral range of energy sources.

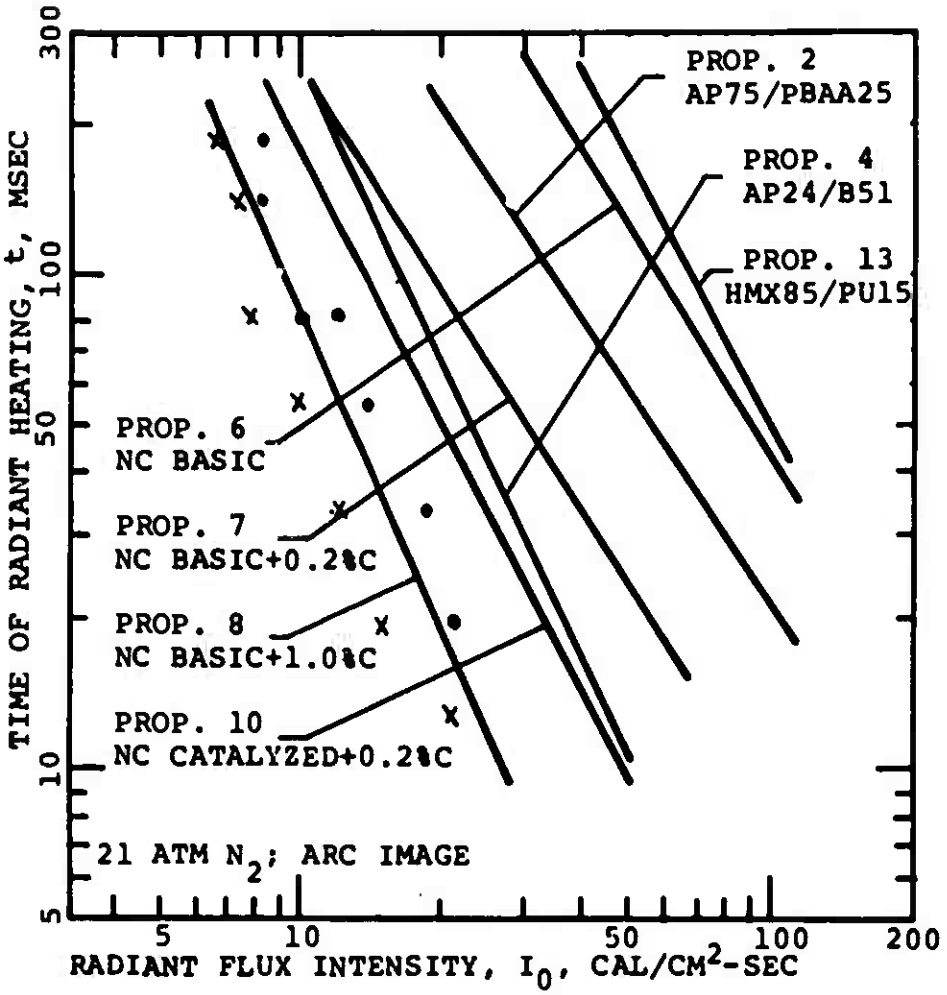

EXAMPLES OF GO/NO-GO DATA FOR PROP. 8 :

✗ FAILURE TO ATTAIN L_{ld} LIMIT

• L_{ld} LIMIT ATTAINED

Fig. 3 Arc image ignition limits of several propellant classes.

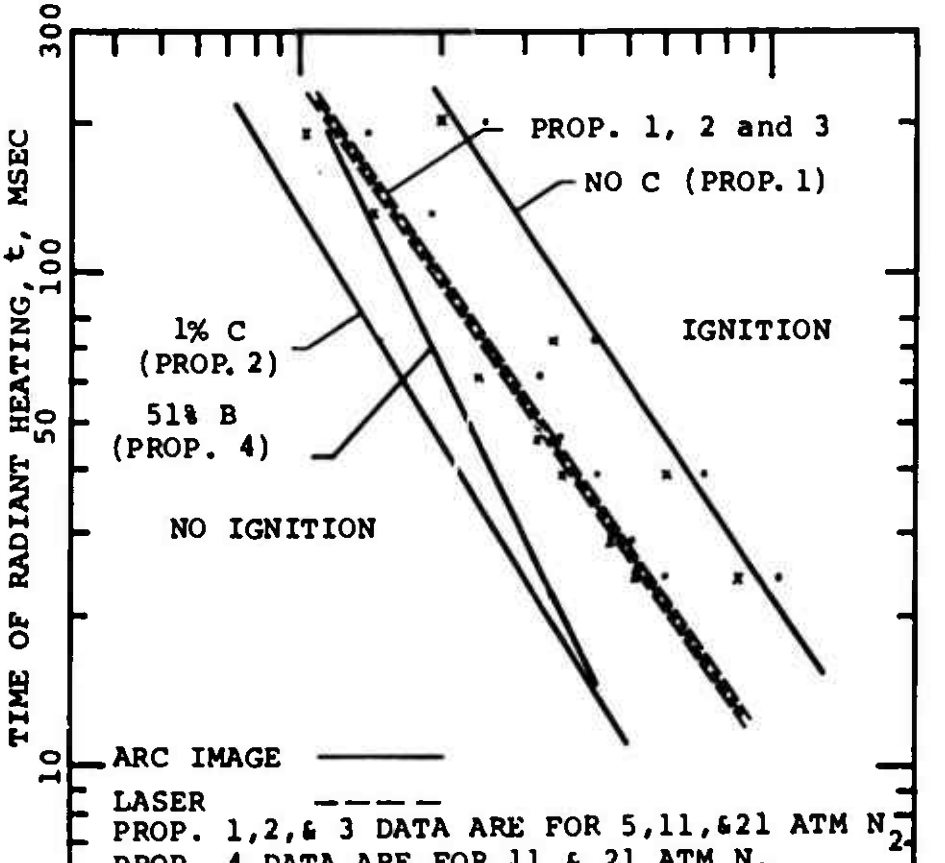

Fig. 4 Ignition of AP composite propellants 1, 2, 3, and 4 demonstrating independence of pressure (Contrast with Fig. 11) and demonstrating that absorbed laser radiation is not affected by carbon powder added to the propellant.

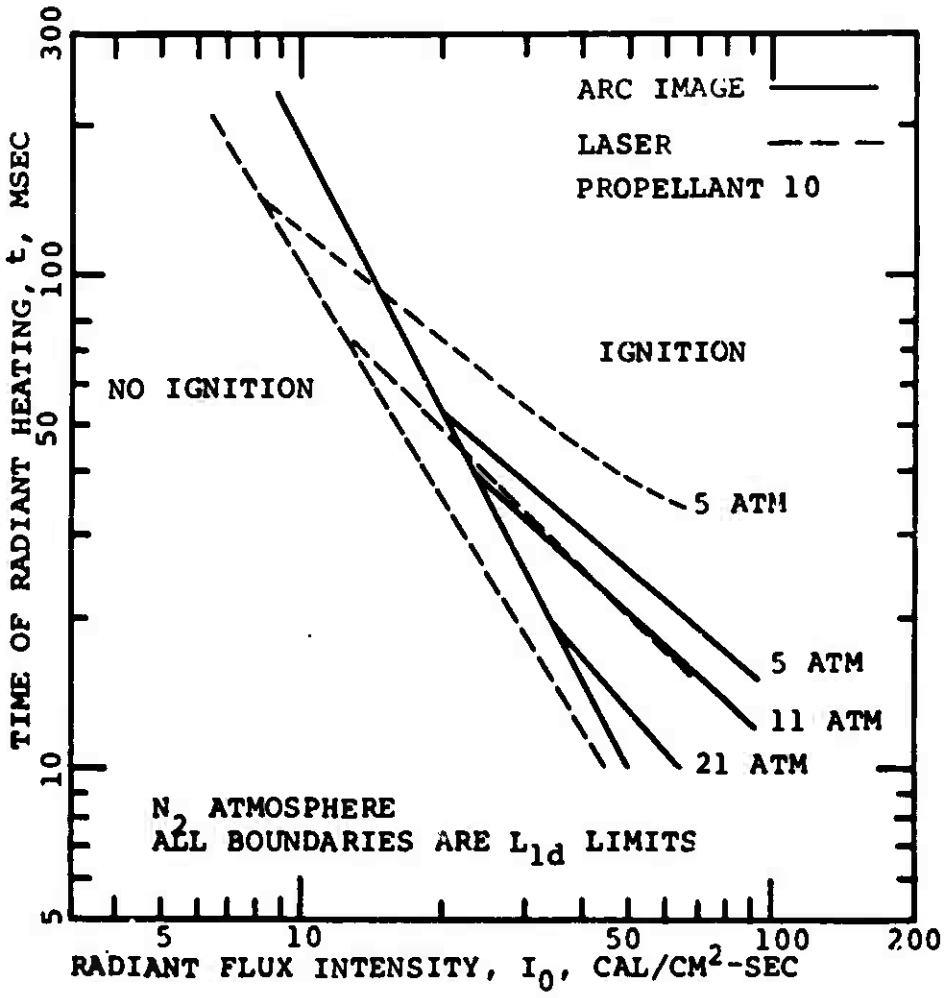

Fig. 5 Catalyzed DB propellant 10 tested in the arc image and laser ignition apparatus showing that pressure sensitivity is characteristic of the propellant not the ignition apparatus.

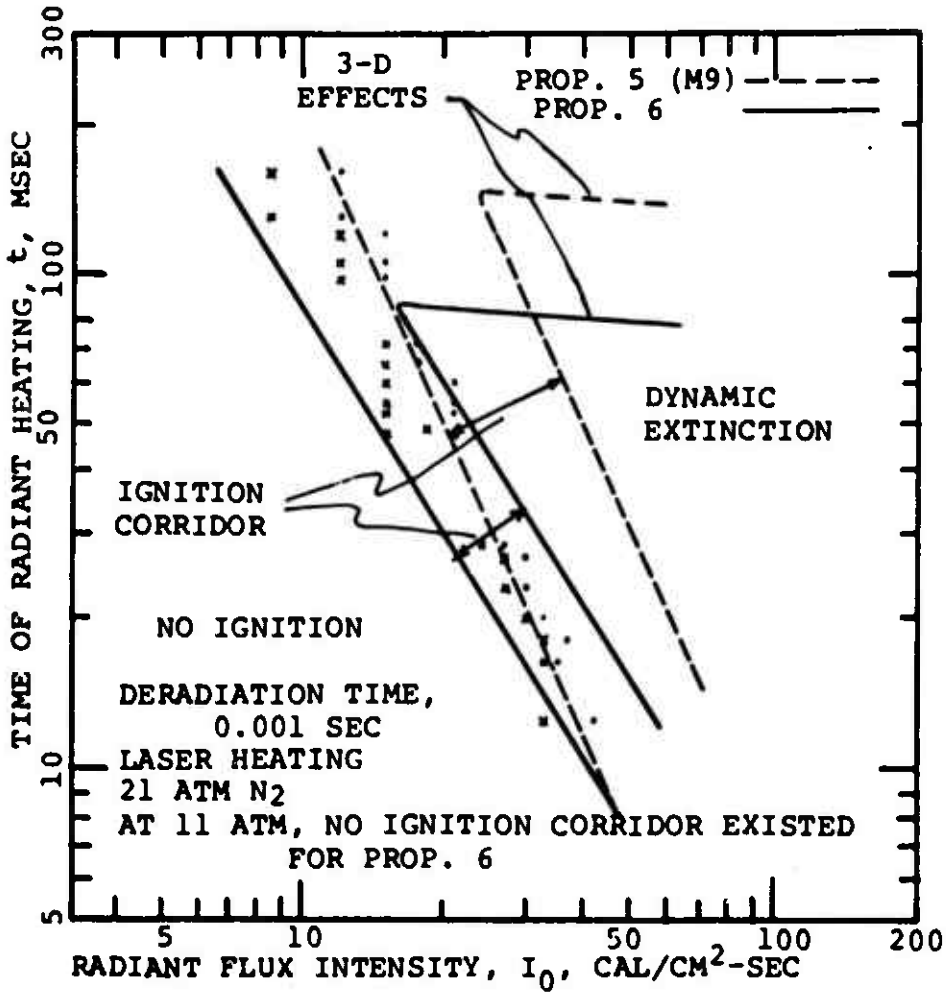

Fig. 6 Dynamic extinction of noncatalyzed DB propellants 5 and 6 tested in the laser ignition apparatus. (No such boundaries noted in arc image tests).

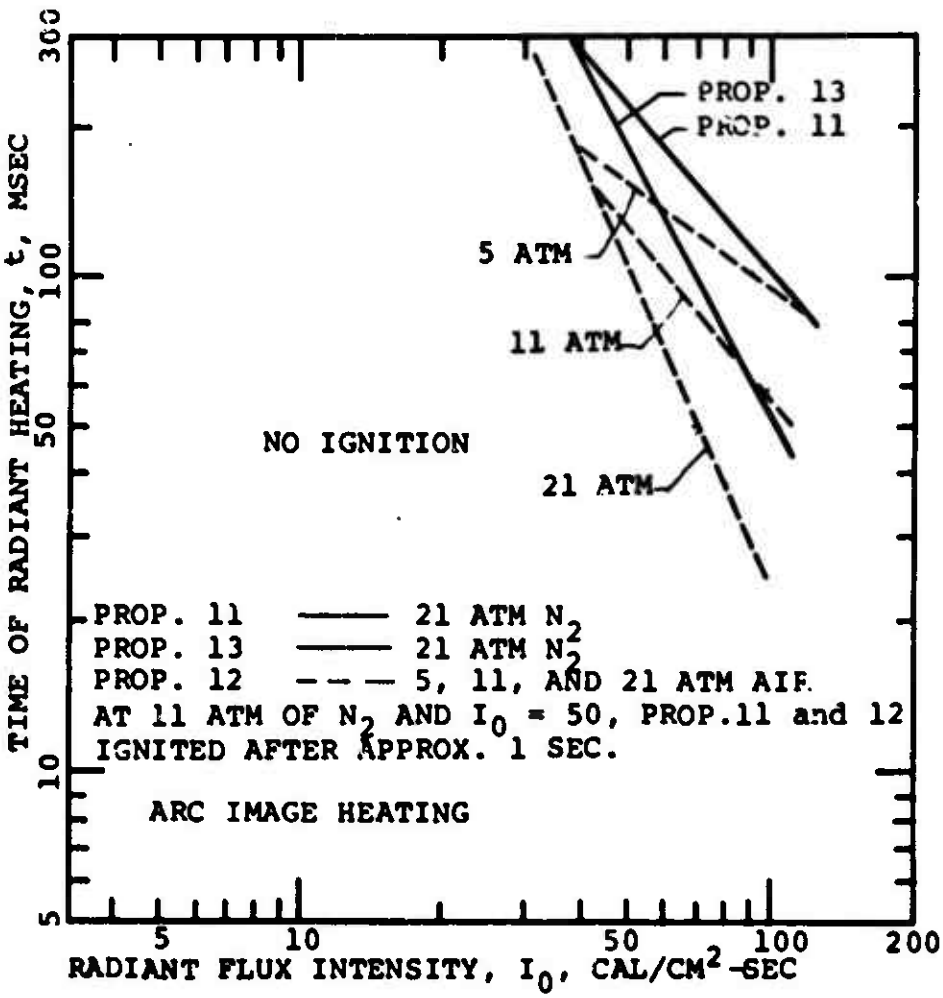

Fig. 7 Arc image ignition data for HMX composite propellants 11, 12, and 13 in nitrogen and in air showing resistance to ignition.

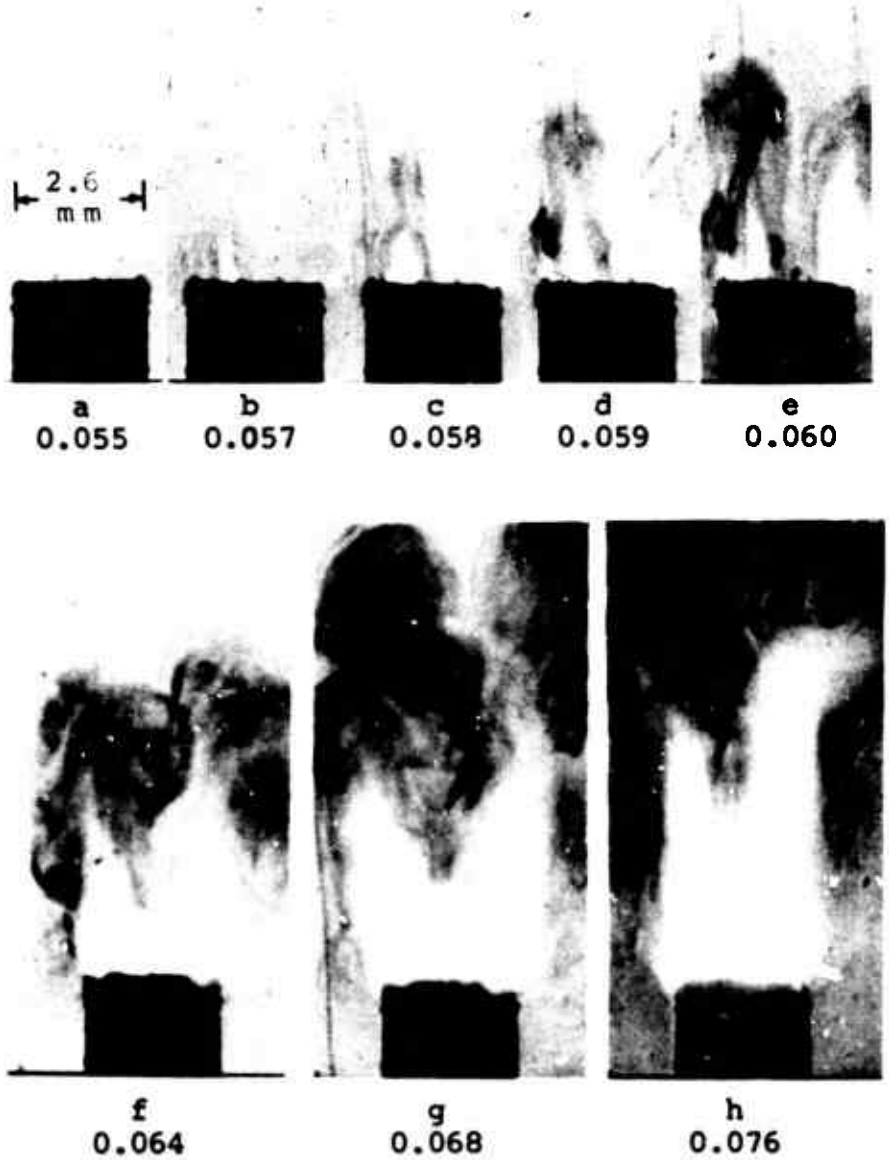

TIMES ARE SECONDS AFTER ONSET OF RADIANT HEATING.
PROPELLANT 1; PRESSURE, 11 ATM N_2;
HEAT FLUX, 30 CAL/CM^2 - SEC

Fig. 8 High speed shadowgraph movie illustrating flame development on AP composite propellants and closely coupled flame.

a
0.007
FIRST
GASIFICATION

b
0.016
DEVELOPING
FLAME

c
0.034
RADIATION
ASSISTED
BURNING

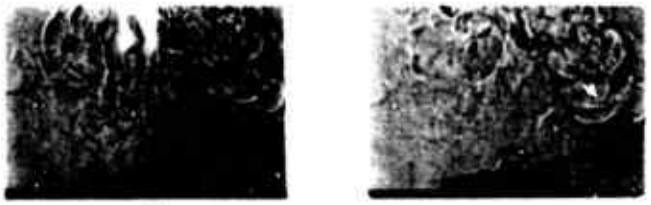

d
0.040
0.004 SEC. AFTER
DERADATION

e
0.047
FLAME
EXTINGUISHED

TIMES ARE SECONDS AFTER ONSET OF
RADIANT HEATING.
PROPELLANT 5; PRESSURE, 21 ATM N_2
HEAT FLUX, 51 CAL/CM^2-SEC

Fig. 9 High speed shadowgraph movie illustrating flame development on noncatalyzed DB propellant showing flame with large stand-off distance.

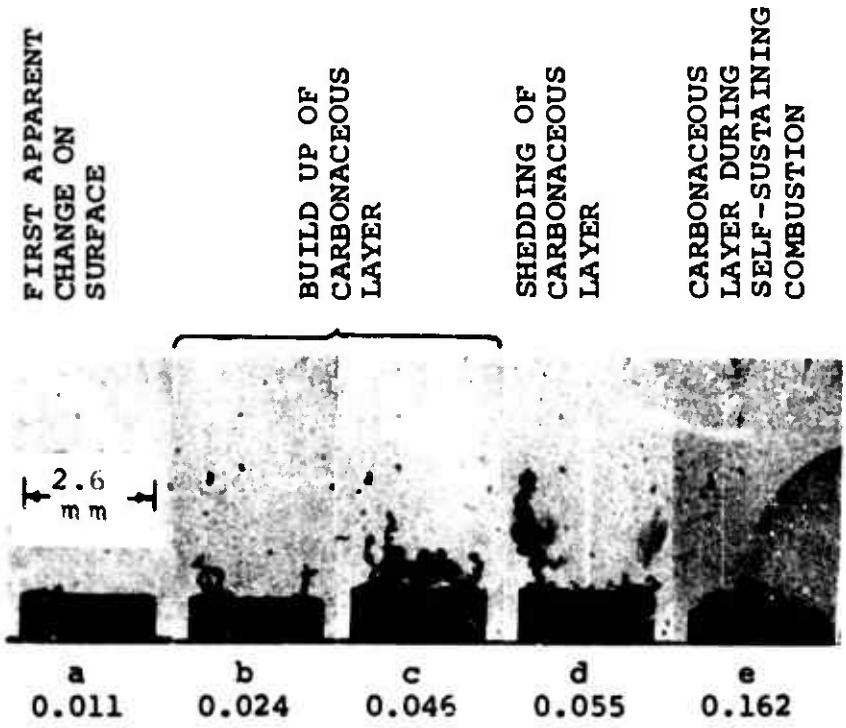

TIMES ARE SECONDS AFTER ONSET OF RADIANT HEATING.
PROPELLANT 9; PRESSURE, 4 ATM N_2;
HEAT FLUX, 42 CAL/CM^2-SEC

Fig. 10 High speed shadowgraph movie showing carbonaceous layer formation on the surface of catalyzed DB propellant.

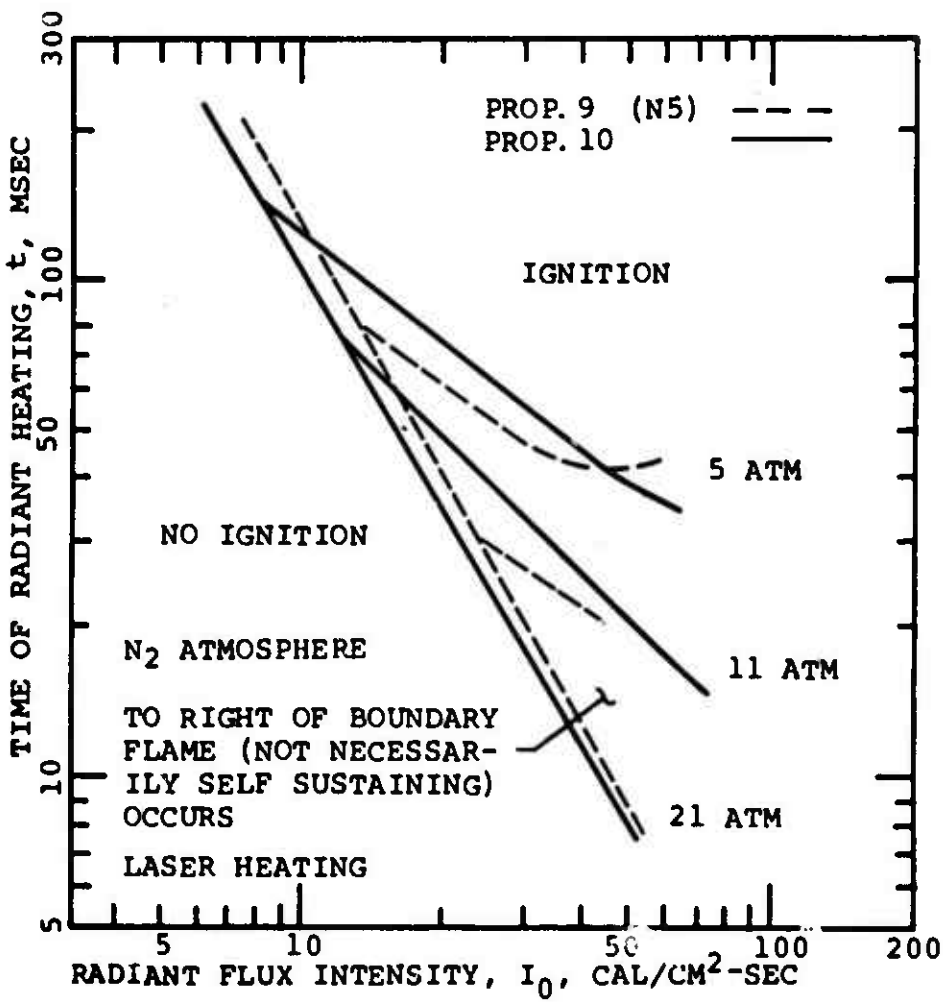

Fig. 11 Catalyzed DB propellants 9 and 10 tested in the laser ignition apparatus showing pressure dependence of ignition boundaries is a property of catalyzed DB propellants.

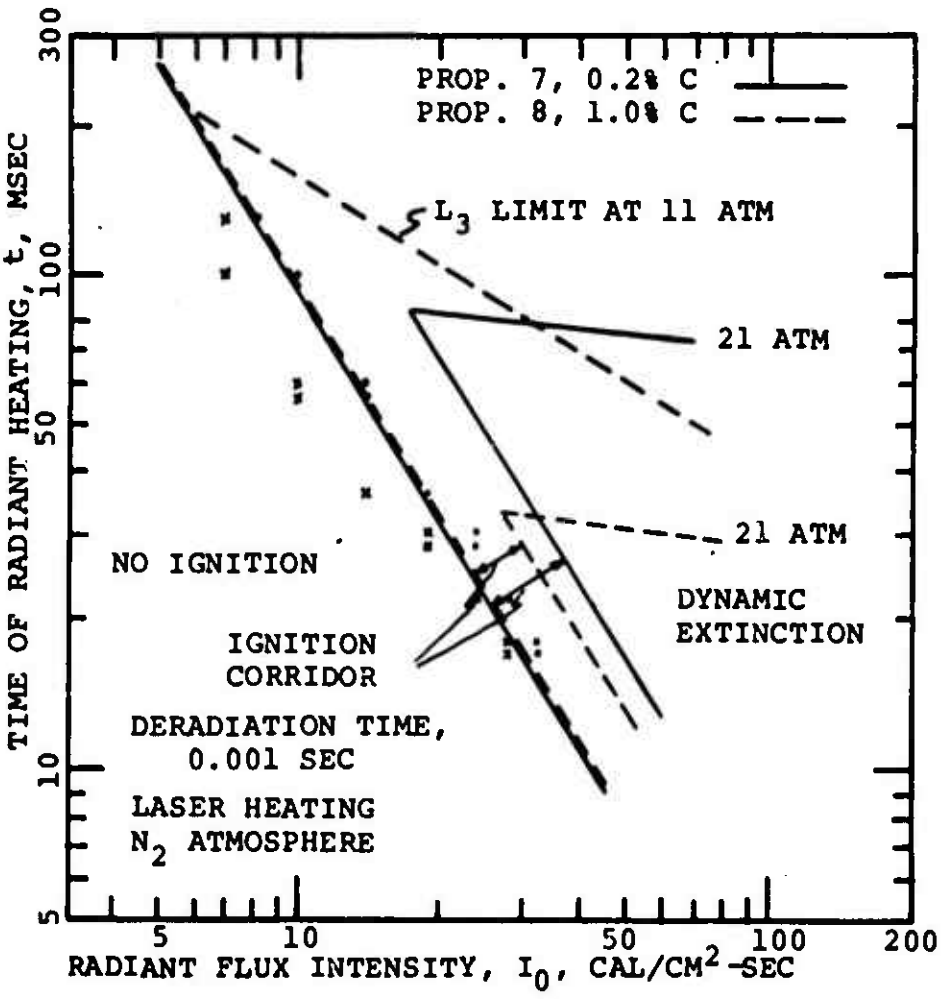

Fig. 12 Addition of carbon reducing dynamic extinction of noncatalyzed DB propellants 7 and 8.

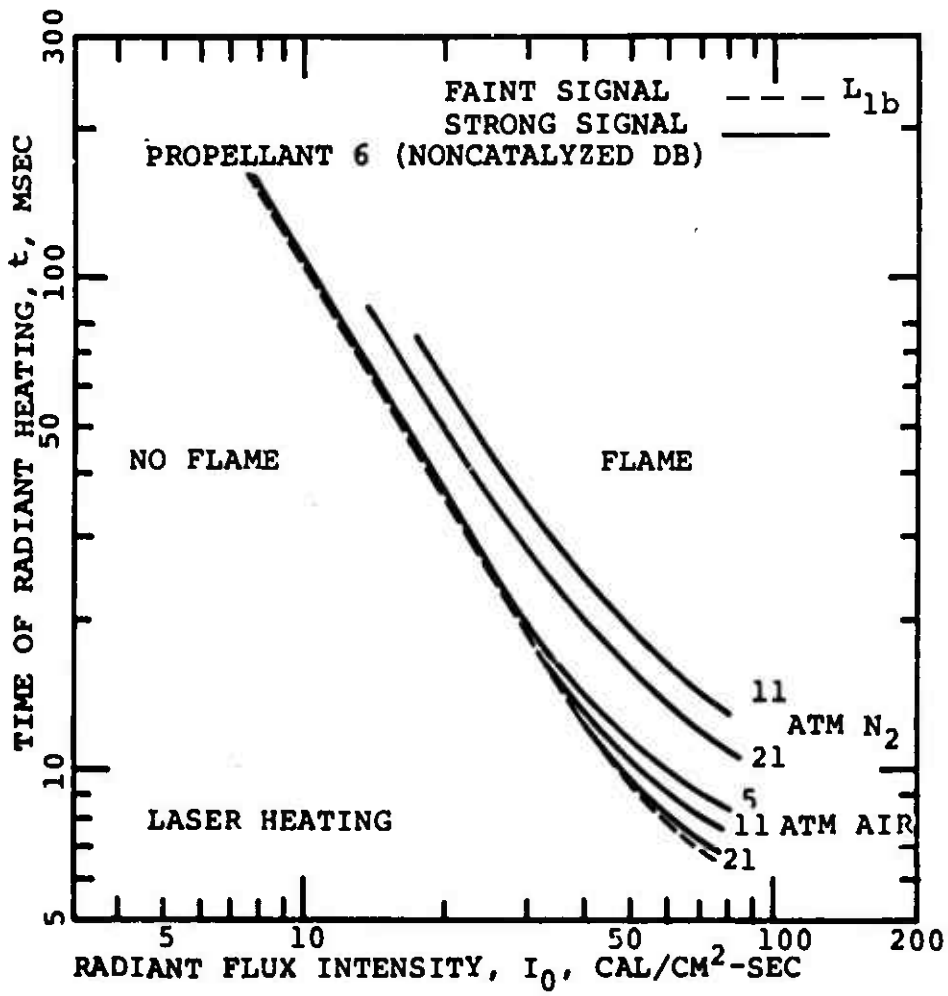

Fig. 13 Pressure dependence of strong surface region IR signal for noncatalyzed DB propellant 6. (Weak signal is independent of pressure and atmosphere.)

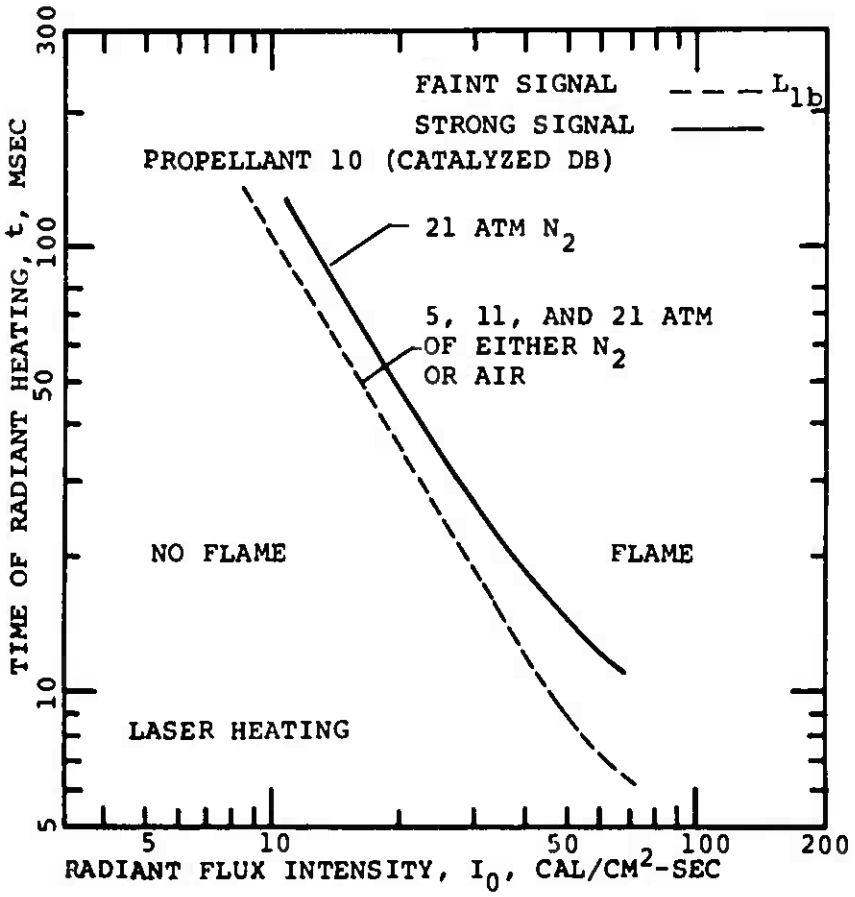

Fig. 14 Pressure independence of initial surface region IR signal for catalyzed DB propellant 10.

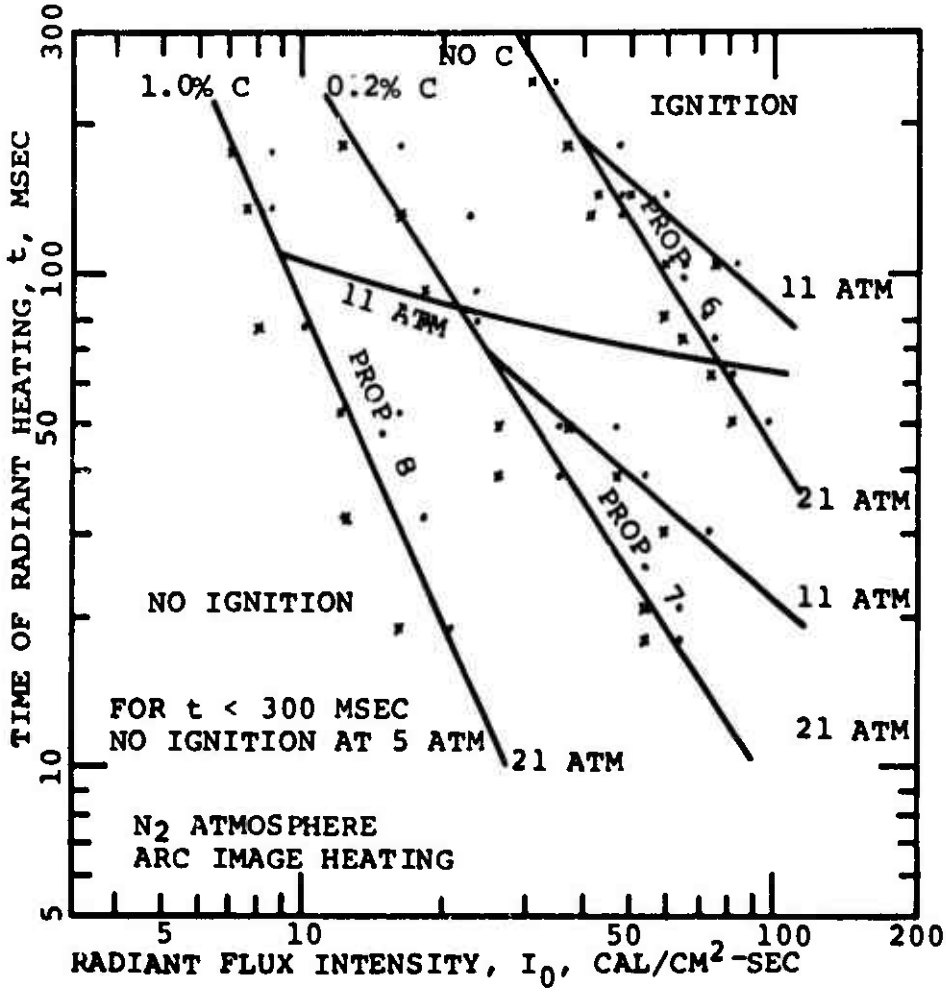

Fig. 15 Arc image ignition data showing decrease of ignition delay with increase of carbon content and absence of dynamic extinction for noncatalyzed DB propellants 6, 7, and 8. (Contrast with Figs. 6 and 12.)

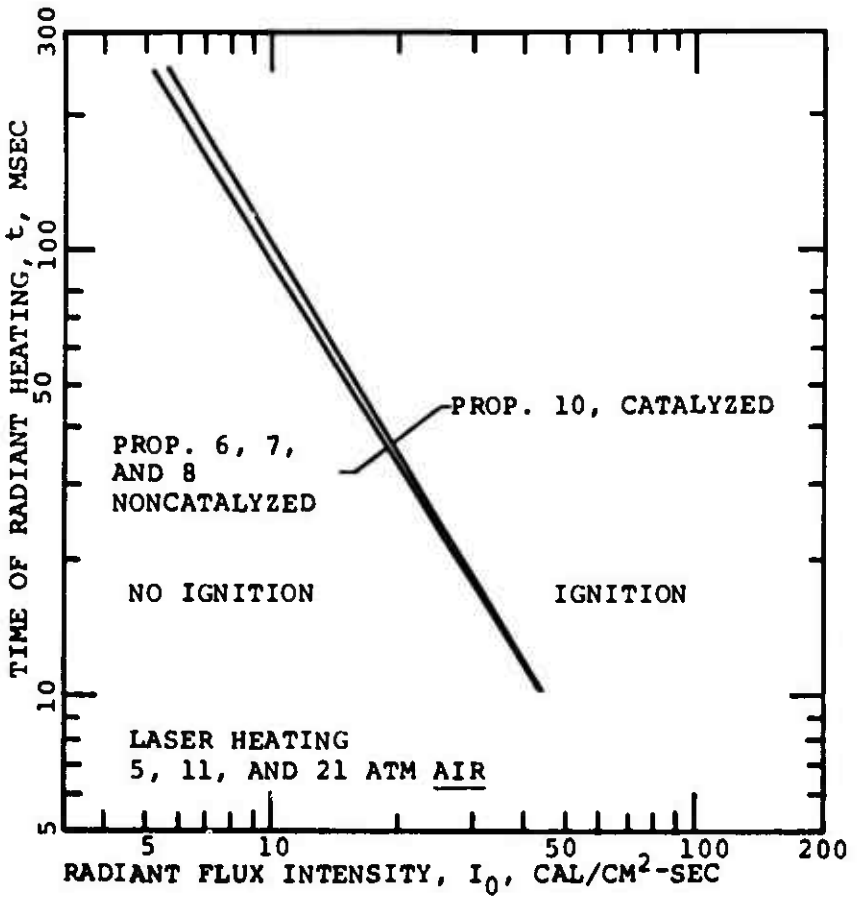

Fig. 16 Noncatalyzed DB propellants 6, 7, and 8, and catalyzed propellant 10 ignited in air showing elimination of pressure dependence.

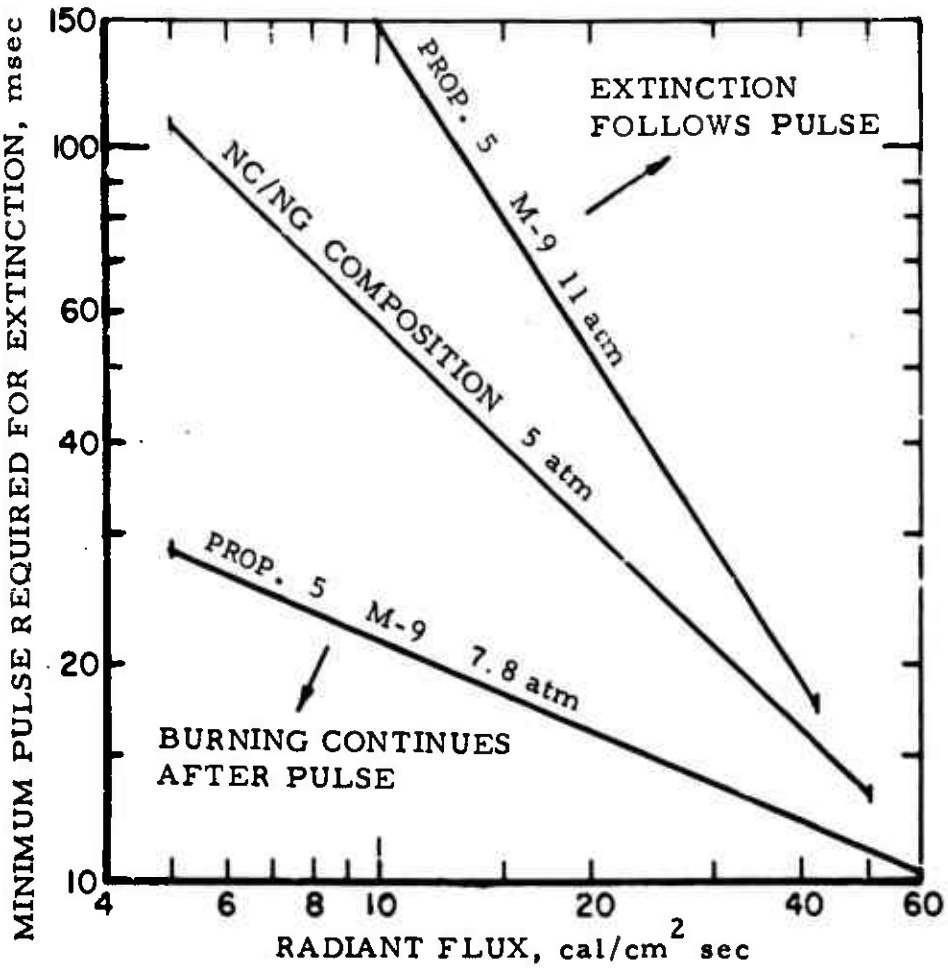

Fig. 17 Measured flux-time extinction boundaries for steadily burning propellant subjected to radiation pulses (deradiation interval 0.002 sec).

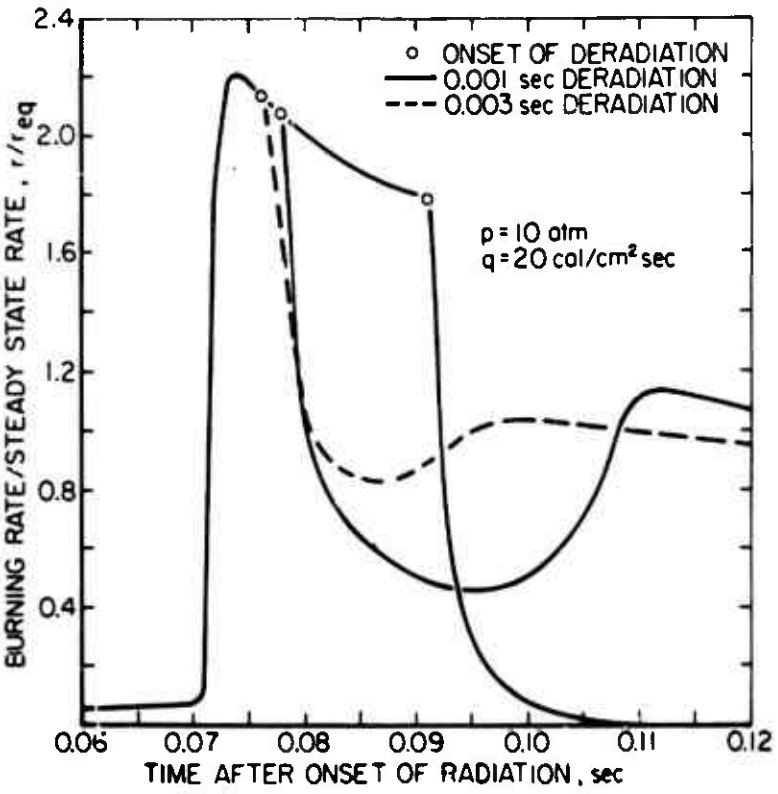

Fig. 18 Calculated burning rate transients with deradiation time and deradiation interval as parameters showing that rapid burning rate transients always follow deradiation.